

Nonparametric quantile regression for time series with replicated observations and its application to climate data

Soudeep Deb*

Indian Institute of Management Bangalore
Bannerghatta Main Rd, Bangalore, KA 560076, India.

and

Kaushik Jana†

Imperial College London
Department of Mathematics,
180 Queen's Gate, London SW7 2AZ, United Kingdom

Abstract

This paper proposes a model-free nonparametric estimator of conditional quantile of a time series regression model where the covariate vector is repeated many times for different values of the response. This type of data is abundant in climate studies. To tackle such problems, our proposed method exploits the replicated nature of the data and improves on restrictive linear model structure of conventional quantile regression. Relevant asymptotic theory for the nonparametric estimators of the mean and variance function of the model are derived under a very general framework. We provide a detailed simulation study which clearly demonstrates the gain in efficiency of the proposed method over other benchmark models, especially when the true data generating process entails nonlinear mean function and heteroskedastic pattern with time dependent covariates. The predictive accuracy of the non-parametric method is remarkably high compared to other methods when attention is on the higher quantiles of the variable of interest. Usefulness of the proposed method is then illustrated with two climatological applications, one with a well-known tropical cyclone wind-speed data and the other with an air pollution data.

Keywords: Air pollution data, Cyclone data, Nadaraya-Watson estimators, Asymptotic normality, Consistency.

*Email: soudeep@iimb.ac.in. ORCID: 0000-0003-0567-7339.

†Email: kaushikjana11@gmail.com. ORCID: 0000-0003-4832-1375

1 Introduction

Replicated data is characterized by many repetitions of the covariate values at different values of the response variable. This is generally denoted by paired data of the form (\mathbf{X}_t, Y_{tj}) , where $j = 1, \dots, n_t$ correspond to different values of the response variable for the t^{th} realization of the covariate vector, i.e. \mathbf{X}_t is replicated n_t times in the dataset. Such data are frequently encountered in many contexts, including climate and environmental science study. For instance, the intensities of tropical cyclones (quantified by maximum wind speed during a particular cyclone) over a period of several years, with multiple observations within a year, have been studied in relation to the year of occurrence and other year-specific climate variables; see for example [Elsner et al. \[2008\]](#), [Jagger and Elsner \[2009\]](#) and [Kossin et al. \[2013\]](#). Time series modelling of daily or sub-daily extreme precipitation levels were related to monthly El Nino Southern Oscillation (ENSO) index values in a few other studies, such as [Nicholls and Kariko \[1993\]](#) and [Ropelewski and Bell \[2008\]](#). Similar problems have been studied in financial time series as well, e.g. [Embrechts et al. \[1997\]](#) analyzed stock returns above a certain threshold in a given time period (say in a year), using the time period as a covariate. On the other hand, in public health growth research, it is common for scientists to study the dependence of certain quantiles of body dimensions on the age, ethnicity, gender etc. of the subject, by using cross-sectional data collected on birthdays of subjects ([Redden et al. \[2004\]](#), [Fernández et al. \[2004\]](#)). It goes without saying that such type of data renders a good opportunity to study the quantiles of the response variable, which is in fact of paramount interest in many environmental problems. The reader is referred to [Huang et al. \[2017\]](#), [Rivas and Gonzalo \[2020\]](#) and [Vasseur and Aznarte \[2021\]](#) for some relevant readings.

For a conventional set up of response-covariate space with the interest in specified quantiles, the linear quantile regression estimator of [Koenker and Bassett Jr \[1978\]](#) can be used for estimating the parameters and related inferences. In the case of replication in the covariate, [Knight \[2001\]](#) and [Jana and Sengupta \[2019\]](#) used an alternative linear quantile regression model for the response sample quantiles at distinct covariate values and studied asymptotic behavior of regression estimates for replicated data. A few more similar applications can be found in [Lu and Fan \[2015\]](#), [Chen et al. \[2021\]](#) and the references therein. Intriguingly, we find that the existing literature always assumes a linear structure in the context of replicated data, albeit it has been well studied that climate data can exhibit highly nonlinear pattern ([Watson-Parris \[2021\]](#)). While it is true that the paucity of the data and only a few distinct values of the covariates can pose a challenge to go beyond linear model, replications offer an option to do better. Furthermore, the time indexing of the variables provide an additional feature of imposing a dependence structure in the modelling. In this paper, we incorporate these features of the data and propose a nonparametric method of estimating conditional quantiles at different levels under a time-dependent framework.

It is of the essence here to give a brief overview of nonparametric techniques in relation to the subject matter of this article. Literature on nonparametric methods in estimating the regression function in a standard setting dates back to more than three decades. The books by [Wahba \[1990\]](#) and [Fan and Gijbels \[2018\]](#) are great resources to understand the introductory theory, while some applications of nonparametric methods in various contexts of climatology can be found in the works by [Lanzante \[1996\]](#), [Henry et al. \[2002\]](#) and [Bercu et al. \[2019\]](#). An attractive advantage of nonparametric approach is that it lets the data to “speak for themselves” and thereby enables one to detect the underlying regression structures in a better way. Naturally, nonparametric methods in the quantile regression problems have also been studied extensively, and several researchers have shown its effectiveness in identifying potentially nonlinear nature of the regression functions in the data. See [Leider \[2012\]](#), [Wei et al. \[2019\]](#) and [Li et al. \[2020\]](#) for some interesting applications of it. These studies, however, do not take into account that the observations can be dependent among themselves, which is often the case for a real-life climate data. To that end, [Honda \[2000\]](#), [Cai \[2002\]](#) and [Ziegelmann \[2005\]](#) are some

of the early papers that derived results on the properties of the quantile estimates of the deterministic component of the underlying process under strong mixing conditions. [Dabo-Niang and Laksaci \[2012\]](#), [Honda \[2013\]](#) and [Gregory et al. \[2018\]](#) are few other crucial improvements in this regard. Interestingly, to the best of our knowledge, the setting of a time series quantile regression with replicated observations has not been considered before. Not only we aim to bridge that gap in this article but we also consider a very general setup that would allow one to use the methods in any such problem. After describing the theoretical properties, we illustrate the usage of the proposed approach through a detailed simulation study as well as two different real data examples related to the climate studies.

Outline of the paper is as follows. The next section describes the notations, main methods and theoretical results. Section 3 presents a simulation study under various setups and we demonstrate the advantages of the nonparametric approach over the existing methods for replicated data. Application and comparison of different methods on two real data sets are illustrated in Section 4. We conclude the main paper with some important remarks in Section 5. Theoretical proofs of the theorems are presented in Section 6 while some additional simulation results are given in Section 7.

2 Methodology

2.1 Notations and existing results

In the following discussion, unless otherwise specified, $\xrightarrow{\mathcal{L}}$ denotes convergence in law, $\mathcal{N}(\eta, \Psi)$ stands for a normal distribution with mean parameter η and dispersion parameter Ψ , $|S|$ denotes the cardinality of a set S , and $\|\cdot\|$ refers to the \mathcal{L}_2 norm. Recall that the \mathcal{L}_p norm for the q -dimensional vector $w = (w_1, w_2, \dots, w_q)^T$ is defined as

$$\|w\|_p = \left(\sum_{i=1}^q |w_i|^p \right)^{1/p}. \quad (2.1)$$

Let \mathbb{N}, \mathbb{Z} denote the set of natural numbers and the set of integers respectively. Throughout this study, we consider time-dependent data of the form $(\mathbf{X}_t, Y_{tj})_{1 \leq t \leq n, j \in \Gamma_t}$, where Γ_t denotes the index set (possibly unobserved) for the replicated observations at time t . Following is the regime we shall consider for developing the asymptotic theory in this work.

Assumption 1. *The index set Γ_t at time t , for $1 \leq t \leq n$, satisfies the condition $|\Gamma_t| \rightarrow \infty$ as $n \rightarrow \infty$.*

In other words, we assume that there are large number of replications at every time point as the size of the data grows. It is also assumed that for a given covariate profile \mathbf{X}_t , Y_{tj} 's are conditionally independent with the common distribution F_t . For $\tau \in (0, 1)$, the τ -quantile of F_t can be written as $q(\tau | \mathbf{X}_t) = \inf\{y : P(Y_{tj} \leq y | \mathbf{X}_t) \geq \tau\}$. The corresponding sample τ -quantile of the observations is then defined as

$$Q_t^{(\tau)} := \hat{q}(\tau | \mathbf{X}_t) = \arg \min_{m_t} \sum_{j \in \Gamma_t} \rho_\tau(Y_{tj} - m_t). \quad (2.2)$$

where $\rho_\tau(u) = u(\tau - I(u < 0))$.

Consider the following quantile regression model [[Koenker, 2005](#)] at probability level $\tau \in (0, 1)$

$$Q_t^{(\tau)} = \mu(\mathbf{X}_t) + \sigma(\mathbf{X}_t)F^{-1}(\tau), \quad (2.3)$$

where $\mu(\cdot)$ and $\sigma^2(\cdot)$ are the mean function and the variance function, $F(\cdot)$ is an appropriately chosen error distribution, and $F^{-1}(\tau)$ denotes the quantile of it at level τ . In particular, when $\mu(\cdot)$ is a linear function and $\sigma(\cdot)$ is constant, it is similar to the standard quantile regression model, hereafter

abbreviated as SQRM. Let β_τ be the coefficient vector for SQRM such that $\mu(\mathbf{X}_t) = \mathbf{X}'_t \beta_\tau$, $\tau \in (0, 1)$, then β_τ can be estimated as (Koenker and Bassett Jr [1978])

$$\hat{\beta}_{\tau;kb} = \arg \min_{\beta} \sum_{t=1}^n \sum_{j \in \Gamma_t} \rho_\tau(Y_{tj} - \mathbf{X}'_t \beta). \quad (2.4)$$

Detailed discussion on this can be found in Koenker [2005]. In a lot of studies, SQRM has been used effectively to analyze climate data, see Jagger and Elsner [2009], Ying et al. [2011] for example. Note that this benchmark method can be naturally applied under the setup of replicated observations.

In the framework of replicated data, Jana and Sengupta [2019] improved upon the above estimate in an asymptotically efficient sense. They used the asymptotic distribution for $Q_t^{(\tau)}$ to propose the following weighted least squares estimate for β_τ :

$$\hat{\beta}_{\tau;js} = \left(\mathbf{X}' \hat{\Omega}_\tau^{-1} \mathbf{X} \right)^{-1} \mathbf{X}' \hat{\Omega}_\tau^{-1} \mathbf{Q}^{(\tau)}. \quad (2.5)$$

In the above expression, $\mathbf{X} = [\mathbf{X}_1 : \dots : \mathbf{X}_n]'$, $\mathbf{Q}^{(\tau)} = (Q_1^{(\tau)}, \dots, Q_n^{(\tau)})'$ and $\hat{\Omega}_\tau$ is a consistent estimate of the diagonal matrix Ω_τ with t^{th} diagonal element as

$$(\Omega_\tau)_{t,t} = \frac{\tau(1-\tau)}{|\Gamma_t| f_t^2(F_t^{-1}(\tau))},$$

where $f_t(\cdot)$ is the density of $F_t(\cdot)$, the error distribution associated with the t^{th} observation.

Theorem 2.1 (Due to Jana and Sengupta [2019]). *Let $N = \sum |\Gamma_t|$ and assume that as $N \rightarrow \infty$ the vector $(|\Gamma_t|/N)_{1 \leq t \leq n}$ converges in Euclidean norm to a vector $(\xi_t)_{1 \leq t \leq n}$ with positive components. F_t , for $1 \leq t \leq n$, are considered to be absolutely continuous, with continuous density function f_t uniformly bounded away from 0 and ∞ at $F_t^{-1}(\tau)$. Let $\max_t \|\mathbf{X}_t\| = o(\sqrt{N})$ and assume that the sample matrices $D_{jn} = N^{-1} \sum_{t=1}^n |\Gamma_t| \{f_t(F_t^{-1}(\tau))\}^j \mathbf{X}_t \mathbf{X}'_t$, for $j = 0, 1, 2$, converge to positive definite matrices D_j , as $N \rightarrow \infty$. Then, the following results hold.*

- (a) $\sqrt{N}(\hat{\beta}_{\tau;kb} - \beta_\tau) \xrightarrow{\mathcal{L}} \mathcal{N}(\mathbf{0}, \tau(1-\tau)D_1^{-1}D_0D_1^{-1})$.
- (b) $\sqrt{N}(\hat{\beta}_{\tau;js} - \beta_\tau) \xrightarrow{\mathcal{L}} \mathcal{N}(\mathbf{0}, \tau(1-\tau)D_2^{-1})$.
- (c) *The limiting dispersion matrix of $\sqrt{N}(\hat{\beta}_{\tau;kb} - \beta_\tau)$ is larger than or equal to that of $\sqrt{N}(\hat{\beta}_{\tau;js} - \beta_\tau)$ in the sense of Löwner order.*

Proof of the above theorem is available on the aforementioned paper and is omitted from here for brevity. The result establishes the superiority of the updated method over the conventional method in an asymptotic sense. The authors also presented detailed simulation study and an application to climate data to demonstrate that $\hat{\beta}_{\tau;js}$ serves as a better estimator for the higher quantiles. Later in this paper, we shall compare the performance of our proposed method against these two benchmark approaches (quantile analysis through $\hat{\beta}_{\tau;kb}$ and $\hat{\beta}_{\tau;js}$) and will refer to them as KB and JS methods, respectively.

2.2 Main assumptions and proposed method

As we pointed out in the introduction, the aforementioned standard techniques fall short when $\mu(\cdot)$ and $\sigma(\cdot)$ are expected to deviate from the assumptions of SQRM. Especially, $\mu(\cdot)$ is often nonlinear in case of quantile regression models in climate data, see for example Ding et al. [2017]. Furthermore,

either the structure of replicated data or the temporal dependence is not utilized in the benchmark methods. In our attempt to develop an alternate methodology on that front, we rely on the fact that sample quantiles converge in probability to true quantiles under Assumption 1. Then, for a fixed $\tau \in (0, 1)$, we consider the stochastic regression model

$$Q_t^{(\tau)} = \mu(\mathbf{X}_t) + \sigma(\mathbf{X}_t)e_t, \quad t = 1, 2, \dots, n, \quad (2.6)$$

where e_t are independent and identically distributed (iid) random errors with $\mathbb{E}(e_t) = 0$ and $\mathbb{E}(e_t^2) = 1$. We keep similar notations as before to avoid confusion. Here, $\mu(\cdot)$ and $\sigma^2(\cdot)$ correspond to respectively the mean function and the conditional variance function of the model. $\sigma(\cdot)$ is considered to be strictly positive. Both functions are unknown and need to be estimated. Note that eq. (2.6) is general enough to include the most common linear and nonlinear regression models for the quantiles. We propose to use nonparametric techniques to develop an improvised version of $\mu(\cdot)$ and $\sigma(\cdot)$ in regressing quantiles for replicated data and that is the primary contribution of this work. To that end, we consider a very general class of stationary processes as functions of iid random variables for the regressor \mathbf{X}_t . Following are the relevant assumptions.

Assumption 2. Let $\varepsilon_j, j \in \mathbb{Z}$, be iid random variables. Then,

$$\mathbf{X}_i = h(\varepsilon_{i-s}; s \in \mathbb{Z}), \quad i \in \mathbb{Z}, \quad (2.7)$$

where h is a measurable function such that \mathbf{X}_i is well-defined.

Assumption 3. e_t in eq. (2.6) is independent of \mathcal{F}_t , the σ -field generated by $(\dots, \varepsilon_{t-1}, \varepsilon_t)$.

Following the coupling idea of Wu [2005], we next define a dependence measure for \mathbf{X}_t . Let $(\varepsilon'_i)_{i \in \mathbb{Z}}$ be an iid copy of $(\varepsilon_i)_{i \in \mathbb{Z}}$, and let $\varepsilon_i^* = \varepsilon_i$ if $i \neq 0$ and $\varepsilon_0^* = \varepsilon'_0$. We use \mathcal{F}_t^* to denote the sigma-field generated by $(\dots, \varepsilon_{t-1}^*, \varepsilon_t^*)$. Let $G_k(\cdot | \mathcal{F}_t)$ be the conditional distribution function of \mathbf{X}_{t+k} given \mathcal{F}_t and $g_k(\cdot | \mathcal{F}_t)$ be the associated conditional density. $G_k(\cdot | \mathcal{F}_t^*)$ and $g_k(\cdot | \mathcal{F}_t^*)$ are defined similarly. Then, as Wu [2005] pointed out,

$$\theta_t = \sup_x \|g_t(x | \mathcal{F}_0) - g_t(x | \mathcal{F}_0^*)\| \quad (2.8)$$

signifies the contribution of ε_0 in predicting \mathbf{X}_t . Further, let

$$\Theta_n = \sum_{t=1}^n \theta_t, \quad \Theta_\infty = \sum_{t=1}^{\infty} \theta_t. \quad (2.9)$$

Assumption 4. $\Theta_\infty < \infty$, which corresponds to short-range dependent processes.

It is clear that the above setup provides a general and attractive framework. In the following discussion, wherever appropriate, $G(\cdot)$ and $g(\cdot)$ would denote the distribution function and the corresponding density function of \mathbf{X}_t . We estimate $g(\cdot)$ using the kernel density form

$$\hat{g}(x; b_n) = \frac{1}{nb_n} \sum_{t=1}^n K\left(\frac{x - \mathbf{X}_t}{b_n}\right), \quad (2.10)$$

where b_n is a bandwidth sequence such that $b_n \rightarrow 0, nb_n \rightarrow \infty$ for $n \rightarrow \infty$; and $K(\cdot)$ is a kernel function whose properties are given by the following.

Assumption 5. For nonparametric estimation purposes, the kernel functions $K(\cdot)$ used in this study are assumed to be bounded, symmetric, Lipschitz continuous, have bounded derivative and satisfy the conditions $\int K(u) du = 1$, $\phi_K = \int K^2(u) du < \infty$ and $\psi_K = \int u^2 K(u) du < \infty$.

Finally, in developing the asymptotic theory, we shall require some regularity conditions on the behavior of the mean function, the variance function and the above-mentioned density functions.

Assumption 6. For a fixed x and for $\epsilon > 0$, denote the ϵ -ball of x by $B(x, \epsilon)$. We call x to be a favourable point if for some $\epsilon > 0$, $\mu(\cdot)$, $\sigma(\cdot)$ and $g(\cdot)$ have bounded fourth-order derivatives in $B(x, \epsilon)$, $\inf_{B(x, \epsilon)} \sigma(x) > 0$, $\inf_{B(x, \epsilon)} g(x) > 0$ and $\sup_{B(x, \epsilon)} g_1(x | \mathcal{F}_0) < M$ for some constant M .

We now move on to estimating our main model. Since the exact expression of $\mu(\cdot)$ is assumed to be unknown, for the data $(\mathbf{X}_t, Y_{tj})_{1 \leq t \leq n, j \in \Gamma_t}$, we are going to use the Nadaraya-Watson type estimator defined as

$$\hat{\mu}(x; b_n) = \frac{1}{nb_n \hat{g}(x; b_n)} \sum_{t=1}^n K\left(\frac{x - \mathbf{X}_t}{b_n}\right) \arg \min_{m_t} \sum_{j \in \Gamma_t} \rho_\tau(Y_{tj} - m_t). \quad (2.11)$$

The above expression gives us a point estimate of $\mu(\cdot)$. In the theorem below, we state a crucial large sample property of the estimate. On one hand, the theorem provides information regarding the asymptotic bias and consistency of the estimate while on the other, it can be used to construct confidence interval for the mean function. Detailed proof of the theorem is relegated to Section 6.

Theorem 2.2. Let x be a favourable point in the sense of Assumption 6. Then, under Assumptions 1, 2, 3, 4 and 5, as $n \rightarrow \infty$,

$$\sqrt{nb_n} \left(\frac{\sqrt{\hat{g}(x; b_n)}}{\sigma(x) \sqrt{\phi_K}} \right) \left(\hat{\mu}(x; b_n) - \mu(x) - \delta(x; b_n) \right) \xrightarrow{\mathcal{L}} \mathcal{N}(0, 1), \quad (2.12)$$

where $\delta(x; b_n) = b_n^2 \psi_K(\mu''(x) + 2\mu'(x)g'(x)/g(x))$ is the asymptotic bias of the estimate.

One can use the theorem directly to compute the confidence interval for $\mu(x)$. However, that requires either a consistent way of estimating $\delta(x; b_n)$ or more assumptions on $\mu'(x)$ and $\mu''(x)$. In order to avoid that, we follow a jackknife type bias correction procedure, similar to [Wu and Zhao \[2007\]](#). The following corollaries to the above theorem provide us the required result on that note.

Corollary 2.1. For $\lambda > 1$, let $\hat{\mu}_\lambda^*(\cdot; \cdot)$ be defined as

$$\hat{\mu}_\lambda^*(x; b_n) = \frac{\lambda \hat{\mu}(x; b_n) - \hat{\mu}(x; \sqrt{\lambda} b_n)}{\lambda - 1}. \quad (2.13)$$

If $K_\lambda(\cdot)$ is the kernel function satisfying $K_\lambda(u) = (\lambda K(u) - \lambda^{-1/2} K(u/\sqrt{\lambda})) / (\lambda - 1)$, then

$$\sqrt{nb_n} \left(\frac{\sqrt{\hat{g}(x; b_n)}}{\sigma(x) \sqrt{\phi_{K_\lambda}}} \right) \left(\hat{\mu}_\lambda^*(x; b_n) - \mu(x) \right) \xrightarrow{\mathcal{L}} \mathcal{N}(0, 1), \quad (2.14)$$

Corollary 2.2. Let $\hat{\sigma}(x)$ be a consistent estimate of $\sigma(x)$. Then, a $100(1 - \alpha)\%$ confidence interval for $\mu(x)$ is

$$\hat{\mu}_\lambda^*(x; b_n) \pm z_{\alpha/2} \left(\frac{\hat{\sigma}(x) \sqrt{\phi_{K_\lambda}}}{\sqrt{nb_n \hat{g}(x; b_n)}} \right). \quad (2.15)$$

Both corollaries follow directly from Theorem 2.2, and the proofs are trivial. While the above results are true for any $\lambda > 1$, experimentation suggested that $\lambda = 2$ works as good as any other value and this choice also makes the computation convenient for us. Thus, in all applications below, we would use $\hat{\mu}_2^*(x; b_n)$. For notational simplicity, we are going to drop the subscript and write it as $\hat{\mu}^*(x; b_n)$.

Next, in order to implement the above result, we have to find a consistent estimate $\hat{\sigma}(x)$. Observe that $Q_t^{(\tau)} - \hat{\mu}^*(\mathbf{X}_t; b_n)$ is the residual from the model. Thus, a natural estimator of $\sigma^2(x)$ is

$$\hat{\sigma}^2(x; b_n) = \frac{1}{nb_n \hat{g}(x; b_n)} \sum_{t=1}^n K_2 \left(\frac{x - \mathbf{X}_t}{b_n} \right) \left(Q_t^{(\tau)} - \hat{\mu}^*(\mathbf{X}_t; b_n) \right)^2. \quad (2.16)$$

Theorem 2.3. *Let x be a favourable point in the sense of Assumption 6 and let assumptions 1, 2, 3, 4 and 5 to be true. Further assume that $\log n/nb_n^3 \rightarrow 0$. Then, $\hat{\sigma}^2(x; b_n) \rightarrow \sigma^2(x)$ in probability as $n \rightarrow \infty$.*

Proof of this theorem is deferred to Section 6. In the next subsection, we describe the implementation techniques of the method and the evaluation criteria to be used in the applications.

2.3 Implementation

We have established crucial asymptotic results of the nonparametric estimates for $\mu(x)$ and $\sigma^2(x)$. In practice, in order to implement the proposed method, we need to choose b_n and $K(\cdot)$ appropriately.

Recall that, in the calculation of $\hat{g}(x; b_n)$ and $\hat{\mu}(x; b_n)$, the bandwidth sequence needs to satisfy the conditions $b_n \rightarrow 0, nb_n \rightarrow \infty$ as $n \rightarrow \infty$. We also note the additional restriction on the bandwidth sequence in Theorem 2.3 for ensuring consistency of $\hat{\sigma}^2(x; b_n)$. It is easy to observe that all these conditions are actually satisfied if we take $b_n = n^{-1/5}$, one of the most common choices in similar nonparametric studies. Thus, we propose to use this choice in all applications. As we shall see in the following sections, it provides good results in all setups. That being said, one can also take a cross-validation type approach to select the bandwidth sequence in a more objective way. Additionally, we want to point out that the estimates in eq. (2.11) and eq. (2.16) can be potentially computed with different choices of bandwidth sequences. As long as the relevant assumptions are true, the asymptotic results hold.

So far as the kernel function is considered, it has been established in many literature that the estimates are not sensitive to the choice of the kernel. In all our computations, we use the kernel function $K(u) = (3/\pi) \max\{0, (1 - \|u\|^2)\}^2$, which satisfies Assumption 5.

In the remaining sections of the paper, we assess the efficacy of the proposed nonparametric method (NP) along with the other two approaches (KB and JS) mentioned before. Throughout, we compare the performances of the three different estimators of $\mu(x)$, calculated via $x' \hat{\beta}_{\tau; kb}$, $x' \hat{\beta}_{\tau; js}$, and $\hat{\mu}(x, b_n)$, as defined in eq. (2.4), eq. (2.5), and eq. (2.11), respectively. Primarily, the comparison is done through the root mean squared error (RMSE) criteria. Let \mathcal{T}_1 (respectively \mathcal{T}_2) denote the training set (respectively the test set) and suppose $\hat{\mu}(x)$ is the fitted value (respectively the prediction) from a model. Then, the training RMSE is calculated as follows:

$$\text{Training RMSE} = \sqrt{\frac{1}{|\mathcal{T}_1|} \sum_{x \in \mathcal{T}_1} (\hat{\mu}(x) - \mu(x))^2}. \quad (2.17)$$

For evaluating the prediction accuracy, along with the RMSE, we compute the mean absolute percentage error (MAPE) which provides a better idea about the scale of the errors. For the test set \mathcal{T}_2 , the prediction RMSE and the prediction MAPE are defined as

$$\text{Prediction RMSE} = \sqrt{\frac{1}{|\mathcal{T}_2|} \sum_{x \in \mathcal{T}_2} (\hat{\mu}(x) - \mu(x))^2}, \quad (2.18)$$

$$\text{Prediction MAPE} = \frac{1}{|\mathcal{T}_2|} \sum_{x \in \mathcal{T}_2} \left| \frac{\hat{\mu}(x) - \mu(x)}{\mu(x)} \right|. \quad (2.19)$$

All calculations in this paper are done in RStudio version 1.2.5033 (coupled with R version 3.6.2). Computation of the standard quantile regression estimator $\hat{\beta}_{\tau;kb}$ of eq. (2.4) is done through the quantreg package by [Koenker \[2019\]](#).

3 Simulation study

The objective of the simulation study in this paper is two-fold. On one hand, we want to observe how well the three different approaches capture the underlying structure of a data generating process (DGP) while on the other, we want to compare the predictive accuracy of the three methods.

To that end, we consider different DGPs (see Table 1). Here, $\mu(\cdot)$ and $\sigma(\cdot)$ refer to the mean and variance functions as defined in eq. (2.3). First, we consider a SQRM-type structure, where \mathbf{X}_t , for $1 \leq t \leq n$, are assumed to be iid, $\mu(\mathbf{X}_t)$ is a linear function and $\sigma^2(\mathbf{X}_t)$ is constant. Second, we keep the same assumptions for \mathbf{X}_t and $\sigma^2(\mathbf{X}_t)$, but consider a nonlinear function for $\mu(\mathbf{X}_t)$. We call it a nonlinear quantile regression model and abbreviate as NLQRM. Next, we do not consider $\sigma^2(\mathbf{X}_t)$ to be constant, but make it proportional to $|\mathbf{X}_t|$, so as to impose potential heteroskedasticity in the model. This model is hereafter termed nonlinear heteroskedastic quantile regression model (NLHQRM). Finally, we relax the iid assumption on \mathbf{X}_t as well, and generate it from an autoregressive process of order 1. This is a general quantile regression model (GQRM).

Table 1: List of DGPs for the simulation study.

DGP	\mathbf{X}_t	$\mu(\mathbf{X}_t)$	$\sigma^2(\mathbf{X}_t)$
SQRM	iid	linear in \mathbf{X}_t	constant
NLQRM	iid	nonlinear in \mathbf{X}_t	constant
NLHQRM	iid	nonlinear in \mathbf{X}_t	$\propto \mathbf{X}_t $
GQRM	AR(1)	nonlinear in \mathbf{X}_t	$\propto \mathbf{X}_t $

For all of the above DGPs, we use scalar covariates \mathbf{X}_t for all $1 \leq t \leq n$. For notational clarity, let us use X_t to denote the scalar covariate. For the linear functional form $\mu(X_t) = \beta_0 + \beta_1 X_t$, we consider $\beta_0 = 1$, $\beta_1 = 0.4$. The constant for $\sigma^2(\cdot)$ is always taken as 1. In the last three DGPs, we take a quadratic form $\mu(X_t) = \beta_0 + \beta_1 X_t + \beta_2 X_t^2$ for the nonlinear function in covariate, and use $\beta_0 = 2.2$, $\beta_1 = 1.7$, $\beta_2 = -0.5$ to simulate the data. In case of GQRM, the AR(1) process is generated using an autoregressive coefficient of 0.6, and with innovations coming from iid standard normal distributions.

Similar to the real life applications discussed in Section 4, the index set Γ_t for the replicated observations at time t are assumed to be unobserved, but $|\Gamma_t|$ are known. In all of the four cases, we choose a balanced design with $|\Gamma_t| = k$. We observe the results for the three competing methods and compare them for different higher quantiles at probability levels $\tau \in \{0.7, 0.8, 0.9, 0.95\}$. Both n (number of time-points) and k (number of replicates) are varied to check for robustness and to understand the difference between small sample and large sample performances of the three estimators. Most of the choices of the parameter values of this section are in line with the related simulation study conducted by [Jana and Sengupta \[2019\]](#).

As mentioned before, we want to find out how well our proposed approach captures the underlying structure of the DGP and also to evaluate the prediction accuracy of the method. Accordingly, for every experiment, we use the first 80% of the simulated data as the training set and keep last 20% of the observations as the out-of-sample test set. Then, we fit the models on the training set, and use the results to make predictions for the test set. For every such experiment, the RMSE for the training set and the prediction RMSE are calculated. In order to check for robustness, we repeat every experiment 1000 times and report the mean RMSE and the mean prediction RMSE below. We shall also point out the corresponding prediction MAPE to have a better understanding of the scale of the errors.

Note that for the brevity of the paper, we present a comparative discussion on the performance of the three methods across different DGPs and include detailed results only for SQRM and GQRM. All other simulation results can be found in Section 7. In all these results, KB corresponds to the method that uses eq. (2.4), JS is the approach that uses eq. (2.5), and NP stands for our proposed approach corresponding to eq. (2.11).

First, in Table 2 and Table 3, the mean RMSE of the fitted quantiles for all the simulations for SQRM and GQRM respectively, corresponding to different values of n and k , are presented. A couple of interesting phenomena can be observed in these tables. For SQRM, the values are close to each other for all the three methods. For GQRM though, it is evident that the nonparametric method outperforms the other two methods. The RMSE is around 9 times higher in case of KB or JS, and that is true for all values of n . Moreover, the results are similar for all quantiles. On the other hand, for our method, we observe that the RMSE decreases substantially as k increases for every choice of n while for same k , the errors are decreasing at a slower rate for different values of n . This points to the fact that the fit gets much better with more number of replicates. Interestingly, KB and JS method display a similar phenomena for SQRM, but not for GQRM. In fact, even for NLQRM and NLHQRM (refer to Section 7), KB and JS perform similarly as in the case of GQRM. Thus, it is clear that whenever the signal function is assumed to be nonlinear, the performance of the two standard methods suffer and these patterns do not change much even for larger values of n and k .

Table 2: Empirical RMSE (mean taken over 1000 simulations) of fitted quantiles using the three different approaches for different values of τ , K and n , when the data are generated from a SQRM.

τ	Method	$n=30$			$n=50$			$n=100$		
		$k=50$	$k=100$	$k=500$	$k=50$	$k=100$	$k=500$	$k=50$	$k=100$	$k=500$
0.7	KB	0.298	0.272	0.251	0.300	0.273	0.250	0.301	0.273	0.253
	JS	0.297	0.271	0.250	0.299	0.272	0.249	0.300	0.272	0.252
	NP	0.177	0.129	0.082	0.180	0.132	0.083	0.183	0.133	0.083
0.8	KB	0.307	0.278	0.251	0.309	0.277	0.254	0.310	0.279	0.254
	JS	0.304	0.276	0.250	0.306	0.275	0.253	0.307	0.277	0.253
	NP	0.188	0.138	0.087	0.194	0.141	0.088	0.197	0.144	0.089
0.9	KB	0.332	0.290	0.259	0.335	0.294	0.263	0.335	0.295	0.263
	JS	0.324	0.286	0.256	0.326	0.288	0.259	0.326	0.289	0.259
	NP	0.221	0.161	0.099	0.226	0.165	0.102	0.230	0.168	0.103
0.95	KB	0.366	0.315	0.271	0.370	0.318	0.271	0.369	0.319	0.273
	JS	0.351	0.305	0.265	0.352	0.306	0.265	0.351	0.308	0.267
	NP	0.254	0.194	0.118	0.261	0.197	0.122	0.265	0.201	0.124

Turn attention to the prediction performances next. Similar to before, prediction RMSE in different cases for SQRM are depicted in Table 4 and the same for GQRM are shown in Table 5. Here also, we can see that the errors are comparable for the simple model. The prediction RMSE for all three methods are around 0.3, which is equivalent to approximately 10-15% prediction MAPE. However, for GQRM, the nonparametric approach performs at least three times better than the competitors. NP maintains around 10% MAPE in this scenario, but the MAPE for KB and JS are more than 30%. Also, for the NP method, the prediction error diminishes gradually for both n and k whereas it remains stable for the two benchmark methods.

A brief discussion of the results for the other two DGPs (NLQRM and NLHQRM) is of the essence to end this section. For both of these processes, NP method shows an RMSE of around one-fourth of what we see in case of KB or JS methods, and that is true for all combinations of n , k and τ . There also, the RMSE of the nonparametric method improves substantially with larger values of k

Table 3: Empirical RMSE (mean taken over 1000 simulations) of fitted quantiles using the three different approaches for different values of τ , K and n , when the data are generated from a GQRM.

τ	Method	$n=30$			$n=50$			$n=100$		
		$k=50$	$k=100$	$k=500$	$k=50$	$k=100$	$k=500$	$k=50$	$k=100$	$k=500$
0.7	KB	1.790	1.776	1.776	1.787	1.784	1.794	1.793	1.790	1.793
	JS	1.814	1.796	1.793	1.802	1.795	1.803	1.799	1.795	1.799
	NP	0.279	0.272	0.244	0.265	0.237	0.222	0.243	0.208	0.188
0.8	KB	1.809	1.800	1.778	1.798	1.794	1.800	1.797	1.800	1.797
	JS	1.817	1.797	1.784	1.806	1.796	1.799	1.800	1.801	1.798
	NP	0.289	0.266	0.249	0.267	0.244	0.223	0.251	0.219	0.191
0.9	KB	1.813	1.823	1.821	1.804	1.801	1.805	1.784	1.799	1.801
	JS	1.834	1.808	1.794	1.816	1.802	1.792	1.789	1.799	1.796
	NP	0.303	0.278	0.249	0.293	0.257	0.226	0.277	0.233	0.197
0.95	KB	1.821	1.819	1.843	1.807	1.810	1.792	1.784	1.794	1.807
	JS	1.881	1.808	1.808	1.859	1.816	1.788	1.813	1.797	1.799
	NP	0.324	0.289	0.262	0.317	0.279	0.235	0.304	0.255	0.207

Table 4: Prediction RMSE (mean taken over 1000 simulations) for the three different approaches for different values of τ , K and n , when the data are generated from a SQRM.

τ	Method	$n=30$			$n=50$			$n=100$		
		$k=50$	$k=100$	$k=500$	$k=50$	$k=100$	$k=500$	$k=50$	$k=100$	$k=500$
0.7	KB	0.311	0.283	0.259	0.303	0.279	0.258	0.305	0.277	0.255
	JS	0.310	0.283	0.258	0.302	0.278	0.257	0.304	0.276	0.255
	NP	0.201	0.148	0.096	0.192	0.144	0.093	0.190	0.139	0.088
0.8	KB	0.322	0.288	0.259	0.318	0.285	0.262	0.313	0.282	0.257
	JS	0.319	0.286	0.259	0.315	0.283	0.260	0.310	0.280	0.255
	NP	0.214	0.157	0.102	0.208	0.154	0.099	0.205	0.149	0.093
0.9	KB	0.349	0.306	0.267	0.341	0.299	0.266	0.339	0.297	0.264
	JS	0.339	0.300	0.263	0.331	0.293	0.262	0.330	0.292	0.260
	NP	0.250	0.185	0.116	0.244	0.179	0.112	0.239	0.175	0.108
0.95	KB	0.380	0.332	0.281	0.384	0.324	0.273	0.374	0.324	0.276
	JS	0.364	0.323	0.276	0.360	0.312	0.266	0.358	0.311	0.269
	NP	0.288	0.224	0.137	0.284	0.217	0.132	0.276	0.211	0.130

and the performance is good for all quantiles. Prediction-wise as well, NP beats KB and JS by and large, even though the latter two record better accuracy than what we see in GQRM. All in all, it can be said that the proposed nonparametric approach performs consistently better than the existing approaches whenever the DGP deviates from a simple quantile regression model. In fact, we find that for both short term and long term forecasting, the proposed approach has a decided advantage over the standard methods. We omit these results for the interest of space. Refer to Section 7 for detailed results for all of the DGPs.

Table 5: Prediction RMSE (mean taken over 1000 simulations) for the three different approaches for different values of τ , K and n , when the data are generated from a GQRM.

τ	Method	$n=30$			$n=50$			$n=100$		
		$k=50$	$k=100$	$k=500$	$k=50$	$k=100$	$k=500$	$k=50$	$k=100$	$k=500$
0.7	KB	1.879	1.889	1.878	1.860	1.839	1.840	1.824	1.822	1.832
	JS	1.911	1.906	1.898	1.877	1.850	1.853	1.829	1.829	1.836
	NP	0.550	0.498	0.461	0.458	0.418	0.409	0.360	0.342	0.329
0.8	KB	1.900	1.894	1.902	1.860	1.835	1.850	1.816	1.823	1.829
	JS	1.933	1.898	1.911	1.871	1.847	1.861	1.826	1.826	1.832
	NP	0.508	0.530	0.500	0.448	0.420	0.411	0.374	0.336	0.315
0.9	KB	1.936	1.896	1.929	1.847	1.867	1.850	1.814	1.815	1.823
	JS	1.941	1.906	1.904	1.894	1.880	1.853	1.827	1.823	1.829
	NP	0.593	0.526	0.527	0.488	0.453	0.414	0.380	0.365	0.310
0.95	KB	1.913	1.921	1.900	1.848	1.825	1.866	1.811	1.805	1.820
	JS	1.981	1.953	1.901	1.929	1.856	1.882	1.856	1.821	1.822
	NP	0.604	0.543	0.525	0.505	0.491	0.433	0.413	0.377	0.344

4 Application

4.1 Tropical cyclone windspeed data

As the first real application of the proposed method, we re-analyse the tropical cyclone data considered in [Elsner et al. \[2008\]](#). This data has been made publicly available by [Jagger and Elsner \[2006\]](#) and can be downloaded from the website <https://myweb.fsu.edu/jelsner/temp/Data.html>. This satellite based data consists of lifetime maximum wind speed (hereafter denoted as W_{\max} , evaluated in meters per second) for all tropical cyclones in the National Hurricane Center (NHC) best track, recorded over the period of 1899 to 2009. As covariates in the model, we consider annually averaged global Sea-Surface Temperature (SST), and Southern Oscillation Index (SOI). In addition, an intercept term and a linear trend are also used as covariates. It is worth mention that both SST and SOI have been extensively used in modeling cyclones, cf. [Nicholls et al. \[1998\]](#) and [Kang et al. \[2019\]](#). In this data, the two covariates are observed yearly while for every year there are multiple observations for W_{\max} and thus, it is under the framework of our study. Number of replications per year vary up to 47. However, recall that our theory is developed under the assumption of sufficient replicates for every time point. Keeping that in mind, we remove the years where the number of replicates is less than 10. That leads to a total of 104 years of data. Finally, as our main focus is on higher wind speed storms (as in [Elsner et al. \[2008\]](#)) which cause major damages, we consider quantiles at the upper probability levels $\tau \in \{0.7, 0.8, 0.9, 0.95\}$.

In the main analysis, W_{\max} values are transformed to the square-root scale. Several authors (e.g. [Brown et al. \[1984\]](#), [Torres et al. \[2005\]](#)) have argued in detail why this transformation is appropriate in this context. Next, in order to assess both the aspects of inference and prediction, we split the data into training and test sets. Similar to the simulation studies, approximately 20% of the total, that is the last 21 years of data, are kept as the test set. All three methods are fit to the training data using the covariates and then predictions are made for the test set. Accuracy metrics are then computed and presented in [Table 6](#).

We see that the nonparametric approach records uniformly better RMSE in both the training set and the test set. For $\tau = 0.7$, the differences between NP and the other two methods are about 0.1, but the same increases substantially for higher quantiles. For instance, in case of 95% quantile, the prediction RMSE for NP is about 35% better than that of KB method, whereas the JS method

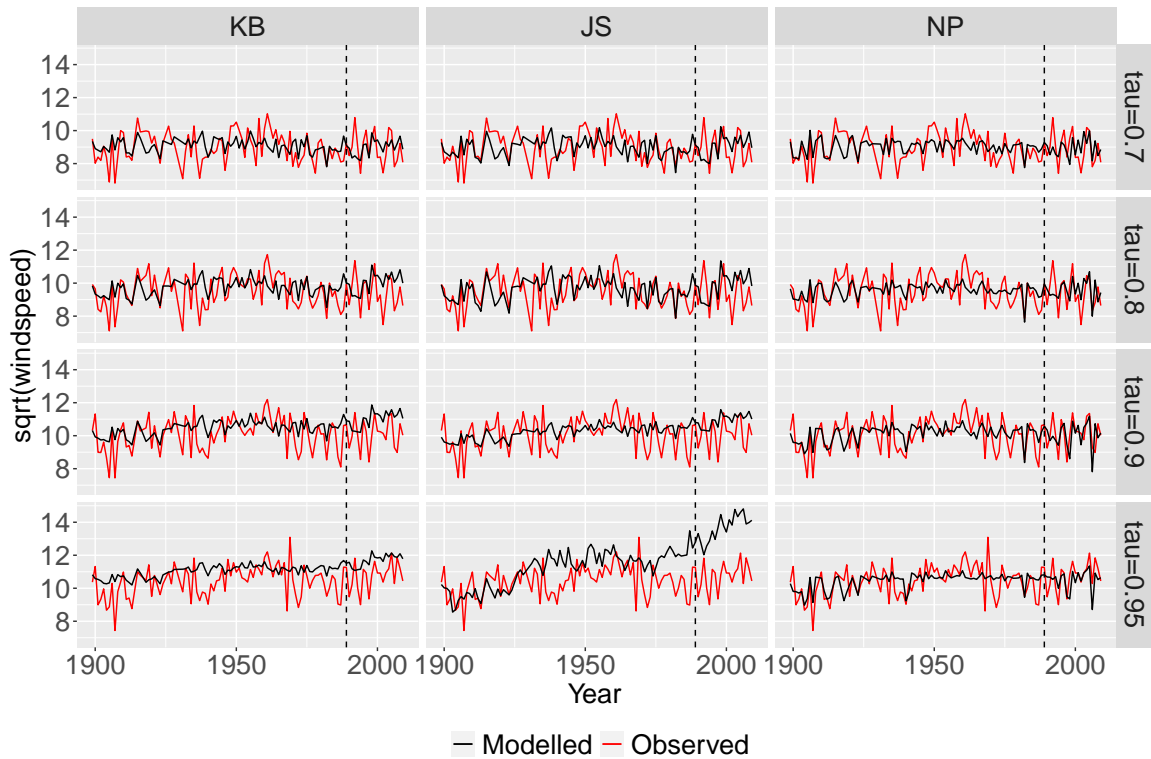
Table 6: RMSE for the fitted quantiles and the overall prediction accuracy (RMSE and MAPE) for the test set, corresponding to different values of τ , from the cyclone data.

τ	Training RMSE			Prediction RMSE			Prediction MAPE		
	KB	JS	NP	KB	JS	NP	KB	JS	NP
0.7	0.889	0.903	0.801	0.905	0.983	0.899	8.66%	9.40%	8.44%
0.8	1.006	1.029	0.888	1.218	1.241	0.931	11.59%	11.56%	8.60%
0.9	1.020	0.976	0.864	1.222	1.153	0.854	10.36%	9.72%	7.16%
0.95	1.097	1.445	0.807	1.185	3.055	0.770	9.87%	27.47%	5.65%

fails miserably. The prediction MAPE values are within 10% in all cases, thereby suggesting that the scales of the errors are not too high. It is necessary to point out that the MAPE for the NP approach decreases for higher quantiles. At $\tau = 0.95$, it is only 5.65%.

Digging deeper into the results, we find that both KB and JS have a tendency to overestimate the mean function. They also fail to capture the peaks and troughs of the data properly, which is not true for our proposed method. It can be observed from Figure 1 where the true series and the fitted series for the three methods are presented. In the figure, results corresponding to the three methods are presented column-wise while the graphs for different quantiles are presented row-wise. The dotted line in each graph represents the beginning of the test period. For both $\tau = 0.7$ and 0.8, all three methods tend to perform at par with each other, but for the extreme quantiles, only the nonparametric approach makes great predictions. It firmly establishes the superiority of the proposed method for higher values of τ .

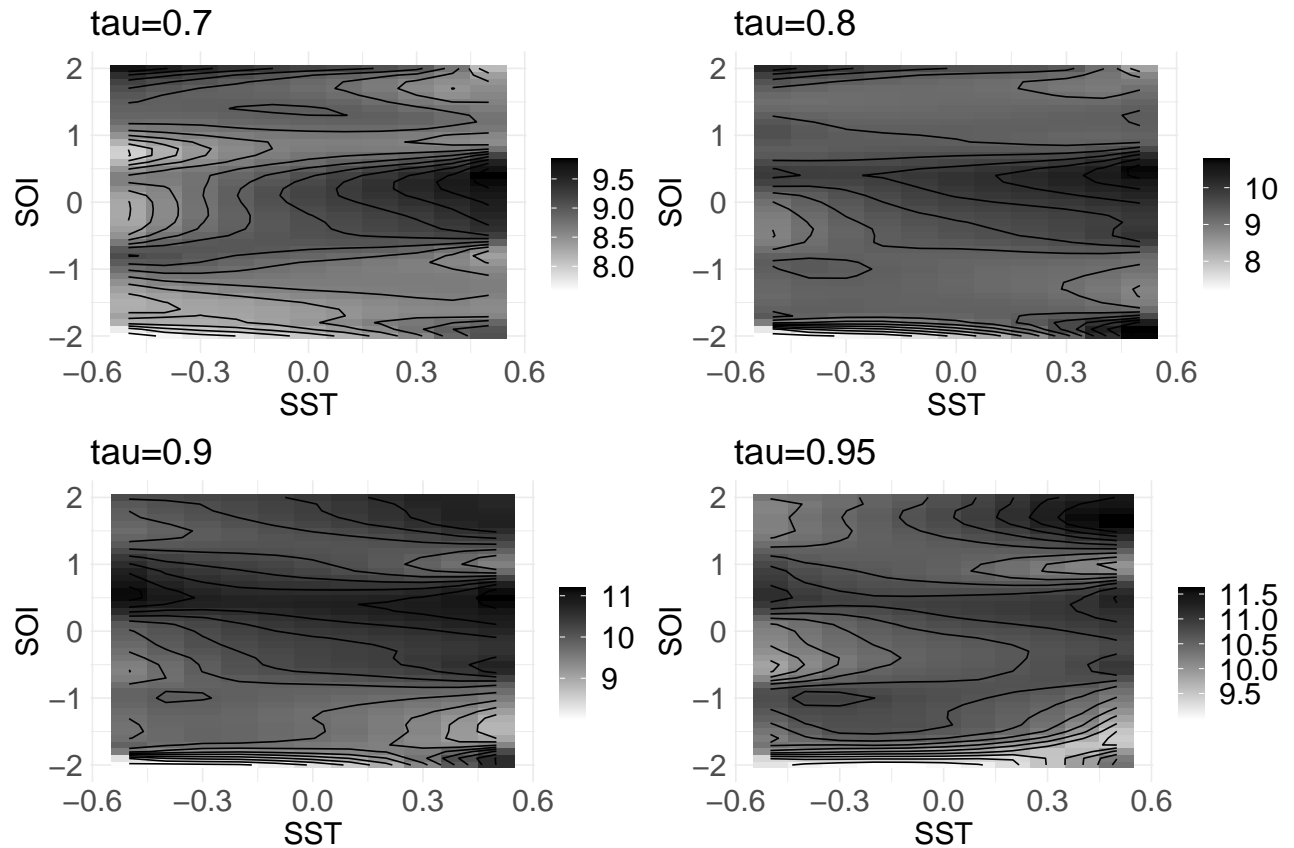
Figure 1: Modelled series for the transformed wind-speed data for different quantiles in the three different approaches. The dotted line represents the beginning of the test period.



To further investigate the results of the nonparametric approach, we take a look at the contour

plot (Figure 2) of the estimated $\mu(x)$ values for different combinations of SST and SOI values at a certain time-point. Remember that both KB and JS assume linearity in the effect of the covariates. However, the contour plot clearly provides strong support in favor of the hypothesis that the mean function is nonlinear in both the regressors at all quantile levels. Along a similar line, we find out that the nonparametric method identifies a nonlinear trend in the data. Moreover, $\sigma(\cdot)$ values for different choices of the covariate levels are estimated to be widely varying. At all quantile levels, it ranges between 0 and 2, which substantiates the use of a general functional form for the conditional variance in our model. Overall, the nonlinear effects of all covariates and the heteroskedastic nature of the variance function are the most plausible explanation of why the proposed approach outperforms the benchmark methods in this application.

Figure 2: Contour plot of the estimated mean function (for the wind-speed data) in the proposed nonparametric method for different choices of the covariate values, corresponding to different quantiles.



Our next analysis is focused to check for robustness of the proposed method in terms of forecasting performance. To that end, we consider different 10-year long forecast periods and evaluate the prediction accuracy metrics in those cases. It should be pointed out that we examined the forecast accuracy for shorter windows as well, and the conclusions were identical. In Table 7, results for five different forecast periods, namely 1991-2000 to 1999-2008 (consecutive periods have two-year shifts), are presented. We notice that for the first three periods, KB method provides best prediction for $\tau = 0.7$, albeit the other two methods are not too worse. For the last two periods in this case, with more data available in the training set, the nonparametric predictions tend to be more accurate. In case of the other quantiles, NP approach consistently performs better. Akin to the previously discussed result, we see that for the largest quantile, the proposed method is by far the best among the competing ones. The MAPE values in case of $\tau = 0.95$ are only about 4 to 6% in NP, whereas KB and JS usually

record close to or more than 10% MAPE. It can be inferred that the benchmark methods work well for lower quantiles, but for the relatively extremes, our proposal has a decided advantage.

Table 7: Prediction RMSE (MAPE given in parentheses) for different forecast periods (10-year window) in the cyclone data.

τ		1991-2000	1993-2002	1995-2004	1997-2006	1999-2008
0.7	KB	0.99 (8.4%)	0.815 (8.4%)	0.855 (8.7%)	0.961 (10.7%)	0.976 (11.2%)
	JS	1.069 (9.1%)	0.865 (8.9%)	0.885 (9.1%)	1.018 (11.4%)	0.982 (11.3%)
	NP	0.991 (8.9%)	0.959 (9.8%)	0.947 (9.4%)	1.002 (10.5%)	0.941 (9.9%)
0.80	KB	1.13 (10.2%)	1.346 (13.6%)	1.257 (11.9%)	1.369 (14%)	1.373 (14.4%)
	JS	1.23 (10.2%)	1.229 (11.9%)	1.201 (11.4%)	1.366 (14.1%)	1.309 (13.9%)
	NP	1.057 (8.8%)	1.013 (9.6%)	0.807 (7.2%)	0.924 (8.8%)	0.963 (9.5%)
0.90	KB	1.183 (10.1%)	1.267 (11.4%)	1.128 (9.3%)	1.239 (10.3%)	1.151 (9.9%)
	JS	1.135 (9.8%)	1.19 (10.7%)	1.062 (8.8%)	1.179 (9.8%)	1.142 (9.7%)
	NP	0.914 (7.5%)	0.831 (7%)	0.69 (5.6%)	0.902 (7.5%)	0.858 (6.5%)
0.95	KB	1.193 (10.3%)	1.311 (11.4%)	1.031 (8.4%)	0.819 (6.5%)	0.839 (7%)
	JS	2.9 (26%)	3.23 (30.1%)	3.164 (28.6%)	3.195 (28.3%)	3.246 (29.1%)
	NP	0.826 (6.6%)	0.693 (5.4%)	0.641 (4.4%)	0.763 (5.8%)	0.569 (4.3%)

4.2 Air pollution data from Bengaluru, India

In this section, we analyze air pollution data from Bengaluru, the capital of the state of Karnataka in India. Bengaluru is one of the fastest growing city in the country. In fact, according to a recent report (London & Partners [2021]), it is the fastest growing mature tech ecosystem in the world since 2016. With this industrial growth and a subsequent boom in population, there has been considerable challenge to maintain good air quality. Naturally, it is of paramount interest to study and forecast the pollution levels in the city, see Abhilash et al. [2018] and Guttikunda et al. [2019] for example.

The data we analyze in this paper is publicly available from the Central Pollution Control Board (website: <https://cpcb.nic.in/>), an official portal of the Government of India. Our main variable in this discussion is related to the particulate matters (PM) with an aerodynamic diameter of less than 2.5 microns. It is measured in micrograms per cubic meter of air. Hereafter, we denote this variable as PM2.5. Several epidemiological studies, such as Jerrett et al. [2005] and Thurston et al. [2016], have established that PM2.5 is linked to a range of serious cardiovascular, respiratory, and other health problems. It is in fact one of the main variables in the study of air pollution.

In case of the data considered in the paper, the measures of PM2.5 are obtained at different hours of a single day from different stations of Bengaluru. As the information of both aspects (hour and location) are not available, it falls within the framework of the current study, where the observations obtained on a single day are considered to be replicated observations at each time point, i.e. on a single day. We use the data from 20th March 2015 to 1st July 2020. For the main analysis, first we remove the cases where the recorded values of the PM2.5 observations are negative, possibly due to erroneous data preparation. We also remove the days where the numbers of replicates are less than a cutoff. That leaves us a total of 1622 days of data. Next, in line with the previous analyses, we use the first 80% time-points in the training set and keep last 20% as the test set. Consequently, we have approximately one year of data in the test set and it helps us to judge the long-term prediction accuracy in the context of the pollution problem.

While carrying out the main analysis, the PM2.5 observations are converted to logarithmic scale using the transformation $x \rightarrow \log(1 + x)$. This is a common pre-processing step in the air pollution

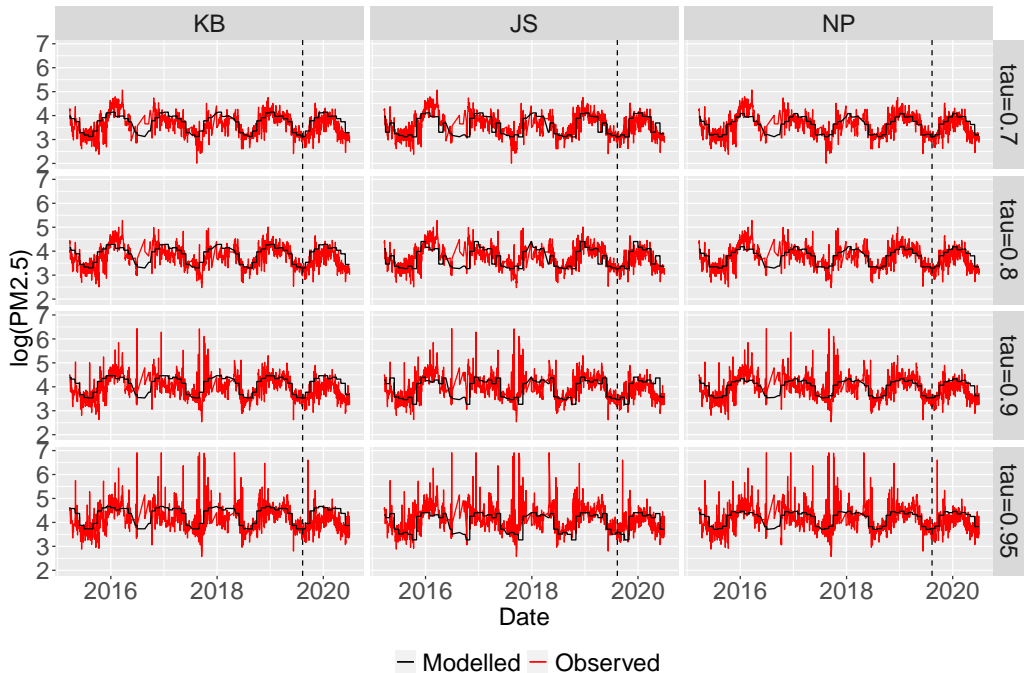
literature, cf. [Smith et al. \[2003\]](#). Moreover, it is imperative to point out that this problem is different from Section 4.1 as we have only time covariates in the data. In order to capture the time-dependence appropriately, we use monthly seasonalities and a common intercept term. We also explored the possibility of including linear and quadratic trends and weekly seasonality terms, but they appeared not to improve the results and are hence omitted from the model.

As before, four different quantiles ($\tau = 0.7, 0.8, 0.9, 0.95$) are considered. For every quantile, all three methods are applied to the training data and predictions are made for the entire test set. We calculate the RMSE from the training set and the prediction RMSE and MAPE from the test set. These values are presented in Table 8. We also plot the entire series along with the modelled series for different methods in Figure 3.

Table 8: RMSE for the fitted quantiles and the overall prediction accuracy (RMSE and MAPE) for the test set, corresponding to different values of τ , from the air pollution data.

τ	Training RMSE			Prediction RMSE			Prediction MAPE		
	KB	JS	NP	KB	JS	NP	KB	JS	NP
0.7	0.345	0.392	0.328	0.446	0.375	0.376	11.19%	8.97%	9.09%
0.8	0.350	0.401	0.332	0.464	0.394	0.380	11.34%	8.97%	8.95%
0.9	0.421	0.481	0.401	0.510	0.478	0.410	12.00%	10.36%	9.35%
0.95	0.495	0.579	0.470	0.584	0.500	0.466	12.92%	9.68%	9.79%

Figure 3: Modelled series for the $\log(\text{PM}_{2.5})$ data for different quantiles in the three different approaches.

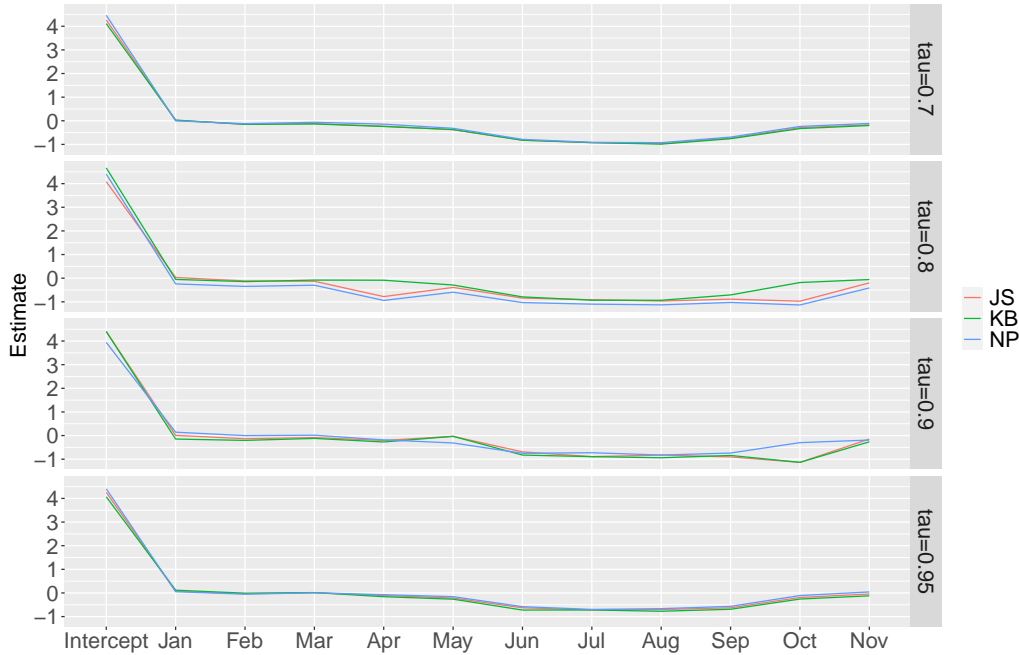


From both Table 8 and Figure 3, it is clear that all three methods fit the data well. The RMSE values are not too different for the training set, although the values corresponding to the JS approach are marginally higher. This pattern, however, does not remain the same in the prediction part. For lower quantiles, we can see that both NP and JS record slightly higher prediction accuracy while for higher quantiles, our proposed approach beats the other two methods by and large. We emphasize

that these differences in the RMSE values are minute and the three methods can be thought to be performing at par with each other. It is in stark contrast with the previous application. A probable explanation is that without any exogenous regressor, all methods would perform similarly. We also hypothesize that the data is more structured in this case and hence, the nonparametric approach provides only minor improvement than the standard approaches.

To better explain the above, observe that the only covariates we use in this analysis are the intercept term and the monthly indicators, which capture the seasonality pattern of the data. Since all of these regressors are binary and non-random quantities, the nonparametric method is in essence similar to KB or JS, as all of them just focus on estimating the effect sizes of the dummy indicators. We present the estimated coefficients in this regard, in Figure 4. From the graph, it is evident that all three methods return almost identical estimates for all of the covariates. This automatically justifies why the methods perform similarly in this application.

Figure 4: Comparison of the coefficient estimates in the three methods for the pollution data, corresponding to different quantiles.



As a last piece of the analysis, in the same spirit as before, we consider different forecast periods to check for robustness. Here, keeping the problem in mind, we explore the performance of the methods for both short-term and long-term prediction. In the context of pollution forecasting, both aspects are important for policymakers and climatologists. In case of the long-term prediction (moving windows of one year) problem, akin to the previous application, we find no discernible difference in the performance of the three methods. Thus, identical conclusions (as in Table 8 and Figure 3) can be drawn for different one-year time windows. However, if we consider one-month windows, mixed results are obtained. Consult Table 9 in this regard. Prediction RMSE and MAPE for the months of January to June in 2020 are displayed. It is evident that there are a couple of months where NP method turns out to be the best, whereas for others JS is producing the best results. KB method is also showing acceptable accuracy. Furthermore, contrary to the earlier finding, we see that the precision of the three methods in different quantiles do not follow any particular pattern here. Hence, overall, the results reconfirm that without the presence of stochastic covariates, all methods can forecast well both

in the short-term and in the long-term.

Table 9: Prediction RMSE (MAPE given in parentheses) for different forecast periods (one-month window) in the air pollution data.

τ		Jan 2020	Feb 2020	Mar 2020	Apr 2020	May 2020	Jun 2020
0.7	KB	0.4 (9%)	0.214 (4.8%)	0.383 (9.2%)	0.586 (16.5%)	0.564 (17.3%)	0.342 (9.7%)
	JS	0.385 (8.6%)	0.216 (4.8%)	0.356 (8.3%)	0.264 (6.8%)	0.516 (15.7%)	0.304 (8.3%)
	NP	0.358 (8%)	0.199 (4.4%)	0.365 (8.7%)	0.493 (13.3%)	0.458 (13.7%)	0.268 (7.1%)
0.8	KB	0.416 (8.9%)	0.245 (5.4%)	0.402 (9.5%)	0.611 (16.7%)	0.579 (17.2%)	0.357 (10.2%)
	JS	0.331 (6.8%)	0.204 (4.4%)	0.363 (8.2%)	0.254 (6.1%)	0.503 (14.8%)	0.294 (7.9%)
	NP	0.345 (7.1%)	0.205 (4.4%)	0.359 (8.2%)	0.502 (13.3%)	0.5 (14.7%)	0.275 (7.3%)
0.9	KB	0.423 (8.8%)	0.295 (6.3%)	0.449 (10.2%)	0.699 (18.5%)	0.655 (18.6%)	0.397 (11%)
	JS	0.287 (5.6%)	0.201 (4.1%)	0.36 (8%)	0.518 (13.2%)	0.883 (25.2%)	0.321 (8.6%)
	NP	0.328 (6.4%)	0.213 (4.3%)	0.351 (7.7%)	0.546 (14%)	0.557 (15.7%)	0.357 (9.8%)
0.95	KB	0.445 (9.1%)	0.319 (6.6%)	0.495 (11%)	0.772 (19.5%)	0.729 (19.7%)	0.442 (11.7%)
	JS	0.304 (5.9%)	0.184 (3.8%)	0.309 (6.2%)	0.43 (10.4%)	0.726 (19.7%)	0.354 (8.7%)
	NP	0.33 (6.3%)	0.208 (4.2%)	0.363 (7.7%)	0.546 (13.3%)	0.606 (16.3%)	0.412 (10.8%)

5 Concluding remarks

In this article, we discuss new ways of modelling time series data with replicated observations, a type of data fairly common in the context of environmental studies. These type of climatological data often exhibit nonlinear mean and heteroskedastic patterns. To model such data, we have proposed a nonparametric approach that leverages sample quantiles of the response variable to estimate quantile function in the presence of covariates. The nonparametric method is kernel based. For a very general framework, under some regularity conditions, we have derived the asymptotic distribution and asymptotic confidence interval of the estimated mean level of the quantile function. We also provided necessary conditions to ensure the consistency of the variance estimates.

Through a detailed simulation study, we have investigated the small sample performance of the three competing methods. Varieties of data generating processes have been considered, ranging from simple linear homoskedastic model to nonlinear (in covariate) heteroskedastic model with time-dependent covariate process and other models in between. We considered different sample sizes and different set of replications reflecting resemblance to the real datasets analyzed in the paper. The performance of the methods are measured with respect to their ability to capture the signal of the data generating process and to evaluate their predictive performances at different future simulated time points. It is observed that for simple linear and homoskedastic data generating process, the performances of the three methods are comparable, but the nonparametric method demonstrates far better performance in both the modelling and the prediction when the data generating process deviates from simplistic model assumptions. The proposed method also exhibits the tendency to capture the information obtained from replicated data with improving efficiency as the number of replication increases, indicating better exploitation of the information in the replicated data. We emphasize that the parametric methods perform at par with the nonparametric approach when the data are generated under the condition that the response does not depend on time-dependent covariates. Otherwise, there is a discernible difference in the efficacy of the proposed method. Interestingly, this difference in the accuracy escalates further for extreme quantiles. The same is observed in the real data analysis as well. For the first application in Section 4.1, where the covariates are time-dependent processes, the gain from nonparametric method is substantial. Contrarily, for the application in Section 4.2, where we do not have information on any time-dependent covariate, this gain is not observed. Overall, the

results support the superiority of the proposed method for higher quantiles in general and it can be used in various climate studies.

Let us conclude the paper with some interesting future directions to this work. Considering that the proposed nonparametric method performs better at reasonably extreme quantiles, it is worth exploring the performance in estimating more extreme situations. Estimation of high return level of random events which cause climate extremes is an important and pressing question which focuses on estimation of probability of rare events based on limited data. Improving the proposed non-parametric method through a suitable mixture kernel by bringing in heavy tailed component would be a suitable method to develop for the estimation of very extreme quantiles. Another potential extension of the current work would be the inclusion of high or infinite dimensional covariates, for instance functions or images, to the model. One case in point is the modelling of the distribution of pivotal environmental variables (such as precipitation regions, as was done in [Jana et al. \[2020\]](#)) at different quantiles using satellite based multiple images as covariates. One can do it through dimension reduction in the covariate space, in conjunction with similar nonparametric techniques. We plan to investigate such problems in future.

Funding sources

The research of the second author is partially supported by the Alan Turing Institute – Lloyd’s Register Foundation Programme on Data-Centric Engineering.

References

- MSK Abhilash, Amrita Thakur, Deepa Gupta, and B Sreevidya. Time series analysis of air pollution in Bengaluru using ARIMA model. In *Ambient Communications and Computer Systems*, pages 413–426. Springer, 2018. 10.1007/978-981-10-7386-1_36.
- Bernard Bercu, Sami Capderou, and Gilles Durrieu. A nonparametric statistical procedure for the detection of marine pollution. *Journal of Applied Statistics*, 46(1):119–140, 2019.
- Barbara G Brown, Richard W Katz, and Allan H Murphy. Time series models to simulate and forecast wind speed and wind power. *Journal of Applied Meteorology and Climatology*, 23(8):1184–1195, 1984.
- Zongwu Cai. Regression quantiles for time series. *Econometric theory*, pages 169–192, 2002.
- I-Chen Chen, Stephen J Bertke, and Brian D Curwin. Quantile regression for exposure data with repeated measures in the presence of non-detects. *Journal of Exposure Science & Environmental Epidemiology*, pages 1–10, 2021. 10.1038/s41370-021-00345-1.
- Sophie Dabo-Niang and Ali Laksaci. Nonparametric quantile regression estimation for functional dependent data. *Communications in statistics-Theory and methods*, 41(7):1254–1268, 2012.
- Qinghua Ding, Axel Schweiger, Michelle L’Heureux, David S Battisti, Stephen Po-Chedley, Nathaniel C Johnson, Eduardo Blanchard-Wrigglesworth, Kirstin Harnos, Qin Zhang, Ryan Eastman, and Eric J Steig. Influence of high-latitude atmospheric circulation changes on summertime arctic sea ice. *Nature Climate Change*, 7(4):289–295, 2017.
- James B Elsner, James P Kossin, and Thomas H Jagger. The increasing intensity of the strongest tropical cyclones. *Nature*, 455(7209):92–95, 2008.
- Paul Embrechts, Claudia Klüppelberg, and Thomas Mikosch. *Modelling Extremal Events*. Berlin: Springer, 1997.

- Jianqing Fan and Irene Gijbels. *Local polynomial modelling and its applications: monographs on statistics and applied probability 66*. Routledge, 2018.
- José R. Fernández, David T. Redden, Angelo Pietrobelli, and David B. Allison. Waist circumference percentiles in nationally representative samples of african-american, european-american, and mexican-american children and adolescents. *The Journal of Pediatrics*, 145(4):439 – 444, 2004.
- Karl B Gregory, Soumendra N Lahiri, and Daniel J Nordman. A smooth block bootstrap for quantile regression with time series. *Annals of Statistics*, 46(3):1138–1166, 2018.
- Sarath K Guttikunda, KA Nishadh, and Pujja Jawahar. Air pollution knowledge assessments (APnA) for 20 Indian cities. *Urban Climate*, 27:124–141, 2019. 10.1016/j.uclim.2018.11.005.
- Ronald C Henry, Yu-Shuo Chang, and Clifford H Spiegelman. Locating nearby sources of air pollution by nonparametric regression of atmospheric concentrations on wind direction. *Atmospheric Environment*, 36(13):2237–2244, 2002.
- Toshio Honda. Nonparametric estimation of a conditional quantile for α -mixing processes. *Annals of the Institute of Statistical Mathematics*, 52(3):459–470, 2000.
- Toshio Honda. Nonparametric quantile regression with heavy-tailed and strongly dependent errors. *Annals of the Institute of Statistical Mathematics*, 65(1):23–47, 2013.
- Q Huang, H Zhang, J Chen, and MJJBB He. Quantile regression models and their applications: a review. *Journal of Biometrics & Biostatistics*, 8(10.4172):2155–6180, 2017.
- Thomas H Jagger and James B Elsner. Climatology models for extreme hurricane winds near the united states. *Journal of Climate*, 19(13):3220–3236, 2006.
- Thomas H Jagger and James B Elsner. Modeling tropical cyclone intensity with quantile regression. *International Journal of Climatology: A Journal of the Royal Meteorological Society*, 29(10):1351–1361, 2009. ISSN 1097-0088. 10.1002/joc.1804.
- K. Jana, D. Sengupta, S. Kundu, A. Chakraborty, and P. Shaw. The statistical face of a region under monsoon rainfall in eastern india. *Journal of the American Statistical Association*, 115:1559–1573, 2020.
- Kaushik Jana and Debasis Sengupta. Improving linear quantile regression for replicated data. *arXiv preprint arXiv:1901.05369*, 2019.
- Michael Jerrett, Richard T Burnett, Renjun Ma, C Arden Pope III, Daniel Krewski, K Bruce Newbold, George Thurston, Yuanli Shi, Norm Finkelstein, Eugenia E Calle, and Michael J Thun. Spatial analysis of air pollution and mortality in los angeles. *Epidemiology*, pages 727–736, 2005.
- Nam-Young Kang, Dongjin Kim, and James B Elsner. The contribution of super typhoons to tropical cyclone activity in response to enso. *Scientific reports*, 9(1):1–6, 2019.
- Keith Knight. Comparing conditional quantile estimators: First and second order considerations. Technical report, Citeseer, 2001. URL <http://citeseerx.ist.psu.edu/viewdoc/download?doi=10.1.1.26.1524&rep=rep1&type=pdf>. University of Toronto working paper.
- Roger Koenker. *Quantile regression*. Cambridge University press, 2005.

- Roger Koenker. *quantreg: Quantile Regression*, 2019. URL <https://CRAN.R-project.org/package=quantreg>. R package version 5.54.
- Roger Koenker and Gilbert Bassett Jr. Regression quantiles. *Econometrica: Journal of the Econometric Society*, 46(1):33–50, 1978.
- James P. Kossin, Timothy L. Olander, and Kenneth R. Knapp. Trend analysis with a new global record of tropical cyclone intensity. *Journal of Climate*, 26(24):9960–9976, 2013.
- John R Lanzante. Resistant, robust and non-parametric techniques for the analysis of climate data: Theory and examples, including applications to historical radiosonde station data. *International Journal of Climatology: A Journal of the Royal Meteorological Society*, 16(11):1197–1226, 1996.
- Julien Leider. A quantile regression study of climate change in chicago, 1960-2010. *Department of Mathematics, Statistics and Computer Science, University of Illinois, Chicago*, 2012.
- Degui Li, Qi Li, and Zheng Li. Nonparametric quantile regression estimation with mixed discrete and continuous data. *Journal of Business & Economic Statistics*, pages 1–16, 2020.
- London & Partners. London: Europe’s global tech city. *DealRoom.co.*, 2021. URL <https://dealroom.co/uploaded/2021/04/dealroom-london-jan-21.pdf>.
- Xiaoming Lu and Zhaozhi Fan. Weighted quantile regression for longitudinal data. *Computational Statistics*, 30(2):569–592, 2015. 10.1007/s00180-014-0550-x.
- Neville Nicholls and Alex Kariko. East Australian Rainfall Events: Interannual Variations, Trends, and Relationships with the Southern Oscillation. *Journal of Climate*, 6(6):1141–1152, 1993. 10.1175/1520-0442(1993)006<1141:EAREIV>2.0.CO;2.
- Neville Nicholls, Chris Landsea, and Jon Gill. Recent trends in australian region tropical cyclone activity. *Meteorology and Atmospheric Physics*, 65(3):197–205, 1998.
- David T. Redden, José R. Fernández, and David B. Allison. A simple significance test for quantile regression. *Statistics in Medicine*, 23(16):2587–2597, 2004. ISSN 1097-0258.
- María Dolores Gadea Rivas and Jesús Gonzalo. Trends in distributional characteristics: Existence of global warming. *Journal of Econometrics*, 214(1):153–174, 2020.
- C. F. Ropelewski and M. A. Bell. Shifts in the Statistics of Daily Rainfall in South America Conditional on ENSO Phase. *Journal of Climate*, 21(5):849–865, 2008. 10.1175/2007JCLI1617.1.
- Richard L Smith, Stanislav Kolenikov, and Lawrence H Cox. Spatiotemporal modeling of pm2. 5 data with missing values. *Journal of Geophysical Research: Atmospheres*, 108(D24), 2003. 10.1029/2002JD002914.
- George D Thurston, Richard T Burnett, Michelle C Turner, Yuanli Shi, Daniel Krewski, Ramona Lall, Kazuhiko Ito, Michael Jerrett, Susan M Gapstur, W Ryan Diver, and C Arden Pope III. Ischemic heart disease mortality and long-term exposure to source-related components of us fine particle air pollution. *Environmental health perspectives*, 124(6):785–794, 2016. 10.1289/ehp.1509777.
- Jose Luis Torres, Almudena Garcia, Marian De Blas, and Adolfo De Francisco. Forecast of hourly average wind speed with arma models in navarre (spain). *Solar energy*, 79(1):65–77, 2005.
- Sebastien Pérez Vasseur and José L Aznarte. Comparing quantile regression methods for probabilistic forecasting of no2 pollution levels. *Scientific Reports*, 11(1):1–8, 2021.

Grace Wahba. *Spline models for observational data*. SIAM, 1990.

D. Watson-Parris. Machine learning for weather and climate are worlds apart. *Phil. Trans. R. Soc. A.*, 379, 2021. ISSN 1364-503X. <https://doi.org/10.1098/rsta.2020.0098>.

Ying Wei, Rebecca D Kehm, Mandy Goldberg, and Mary Beth Terry. Applications for quantile regression in epidemiology. *Current Epidemiology Reports*, 6(2):191–199, 2019.

Wei Biao Wu. Nonlinear system theory: Another look at dependence. *Proceedings of the National Academy of Sciences*, 102(40):14150–14154, 2005.

Wei Biao Wu and Zhibiao Zhao. Inference of trends in time series. *Journal of the Royal Statistical Society: Series B (Statistical Methodology)*, 69(3):391–410, 2007.

Ming Ying, Baode Chen, and Guoxiong Wu. Climate trends in tropical cyclone-induced wind and precipitation over mainland china. *Geophysical Research Letters*, 38(1), 2011.

Zhibiao Zhao and Wei Biao Wu. Kernel quantile regression for nonlinear stochastic models. *Technical ReportNo*, 572, 2006.

Zhibiao Zhao and Wei Biao Wu. Confidence bands in nonparametric time series regression. *The Annals of Statistics*, 36(4):1854–1878, 2008.

Flavio A Ziegelmann. A nonparametric least-absolute-deviations estimator of volatility functions. *XXVII Encontro Brasileiro de Econometria, Natal*, 10, 2005.

6 Proofs

Proof of Theorem 2.2. Note that

$$\frac{\sqrt{nb_n}\sqrt{\hat{g}(x; b_n)}}{\sigma(x)\sqrt{\phi_K}} [\hat{\mu}(x; b_n) - \mu(x)] = \frac{1}{\sigma(x)\sqrt{\phi_K nb_n \hat{g}(x; b_n)}} \sum_{t=1}^n K\left(\frac{x - \mathbf{X}_t}{b_n}\right) \{\mu(\mathbf{X}_t) - \mu(x) + \sigma(\mathbf{X}_t)e_t\} \quad (6.1)$$

Let $r(x; b_n) = g(x)/\hat{g}(x; b_n)$ and

$$S(x; b_n) = \frac{1}{\sigma(x)\sqrt{\phi_K nb_n g(x)}} \sum_{t=1}^n K\left(\frac{x - \mathbf{X}_t}{b_n}\right) \sigma(\mathbf{X}_t)e_t, \quad (6.2)$$

$$B(x; b_n) = \frac{1}{nb_n g(x)} \sum_{t=1}^n K\left(\frac{x - \mathbf{X}_t}{b_n}\right) \{\mu(\mathbf{X}_t) - \mu(x)\}. \quad (6.3)$$

It is easy to observe that eq. (6.1) can be rewritten as

$$\frac{\sqrt{nb_n}\sqrt{\hat{g}(x; b_n)}}{\sigma(x)\sqrt{\phi_K}} [\hat{\mu}(x; b_n) - \mu(x) - r(x; b_n)B(x; b_n)] = \sqrt{r(x; b_n)}S(x; b_n). \quad (6.4)$$

We shall treat the two terms $S(x; b_n)$ and $B(x; b_n)$ separately. First, $S(x; b_n)$ can be written as the sum of $W_t(x; b_n)$ where

$$W_t(x; b_n) = \frac{K\left(\frac{x - \mathbf{X}_t}{b_n}\right) \sigma(\mathbf{X}_t)e_t}{\sigma(x)\sqrt{\phi_K nb_n g(x)}}.$$

Recall Assumption 3 and let \mathcal{G}_t be the sigma-field generated by $(\dots, \varepsilon_{t-1}, \varepsilon_t, \varepsilon_{t+1}; \dots, e_{t-1}, e_t)$. Then, the sequence $\{W_t(x; b_n)\}_{t=1}^n$ form a martingale difference sequence with respect to the filtration \mathcal{G}_t . Next, denoting $c(x) = (\phi_K g(x) \sigma^2(x))^{-1}$, in view of Assumption 2 and the above results, we can write

$$\begin{aligned} \sum_{t=1}^n \mathbb{E}(W_t^2(x; b_n) | \mathcal{G}_{t-1}) &= \frac{c(x)}{nb_n} \sum_{t=1}^n \mathbb{E} \left[K^2 \left(\frac{x - \mathbf{X}_t}{b_n} \right) \sigma^2(\mathbf{X}_t) e_t^2 | \mathcal{G}_{t-1} \right] \\ &= \frac{c(x)}{nb_n} \sum_{t=1}^n K^2 \left(\frac{x - \mathbf{X}_t}{b_n} \right) \sigma^2(\mathbf{X}_t). \end{aligned}$$

Let $u_t = K^2((x - \mathbf{X}_t)/b_n) \sigma^2(\mathbf{X}_t)$. It is easy to work out that, as $n \rightarrow \infty$,

$$\frac{1}{nb_n} \sum_{t=1}^n \mathbb{E}(u_t) \rightarrow \phi_K g(x) \sigma^2(x). \quad (6.5)$$

Further, let $u_t - \mathbb{E}(u_t) = v_t + w_t$, where $v_t = u_t - \mathbb{E}(u_t | \mathcal{F}_{t-1})$, $w_t = \mathbb{E}(u_t | \mathcal{F}_{t-1}) - \mathbb{E}(u_t)$. Observe that $\{v_t\}_{t=1}^n$ form a martingale difference sequence with respect to the filtration \mathcal{F}_t and $\mathbb{E}(v_t^2) = O(b_n)$. Thus,

$$\frac{1}{nb_n} \sum_{t=1}^n v_t \rightarrow 0. \quad (6.6)$$

On the other hand, $w_t = \int K^2(u) \sigma^2(x - ub_n) \{g(x - ub_n | \mathcal{F}_{t-1}) - g(x - ub_n)\} du$. Then, using Lemma 1 from Zhao and Wu [2008], it can be shown that

$$\frac{1}{nb_n} \left\| \sum_{t=1}^n w_t \right\| \rightarrow 0. \quad (6.7)$$

Combining equations (6.5), (6.6) and (6.7),

$$\sum_{t=1}^n \mathbb{E}(W_t^2(x; b_n) | \mathcal{G}_{t-1}) = \frac{c(x)}{nb_n} \sum_{t=1}^n K^2 \left(\frac{x - \mathbf{X}_t}{b_n} \right) \sigma^2(\mathbf{X}_t) \rightarrow 1. \quad (6.8)$$

Next step is to look at the Lindeberg condition for $W_t(x; b_n)$.

$$\begin{aligned} \sum_{t=1}^n \mathbb{E}[W_t^2(x; b_n) \mathbb{I}\{|W_t(x; b_n)| \geq \delta\}] &= \frac{c(x)}{nb_n} \sum_{t=1}^n \mathbb{E} [u_t e_t^2 \mathbb{I}\{|u_t e_t^2| \geq \delta^2 nb_n / c(x)\}] \\ &= \frac{c(x)}{b_n} \mathbb{E} [u_0 e_0^2 \mathbb{I}\{|u_0 e_0^2| \geq \delta^2 nb_n / c(x)\}]. \end{aligned}$$

Under the aforementioned assumptions, u_0 is independent of e_0 , $\mathbb{E}(u_0) = O(b_n)$ and $\sup |u_0| \leq M$ for some finite constant M and for large enough n . Thus, $\mathbb{I}\{|u_0 e_0^2| \geq \delta^2 nb_n / c(x)\} \leq \mathbb{I}\{|e_0^2| \geq \delta^2 nb_n / M c(x)\}$, which further implies that $\mathbb{E}[e_0^2 \mathbb{I}\{|u_0 e_0^2| \geq \delta^2 nb_n / c(x)\}] \rightarrow 0$ as $n \rightarrow \infty$. Clearly, as $n \rightarrow \infty$, the following Lindeberg condition holds.

$$\sum_{t=1}^n \mathbb{E}[W_t^2(x; b_n) \mathbb{I}\{|W_t(x; b_n)| \geq \delta\}] \rightarrow 0. \quad (6.9)$$

Hence, using martingale central limit theorem, we can say that $S(x; b_n) \rightarrow \mathcal{N}(0, 1)$.

We now turn our attention to $B(x; b_n)$. Keeping the notations same as above for convenience, let $u_t = K((x - \mathbf{X}_t)/b_n) \{\mu(\mathbf{X}_t) - \mu(x)\}$. Similarly as above, we write it as $u_t = v_t + w_t + E(u_t)$ where

$v_t = u_t - \mathbb{E}(u_t | \mathcal{F}_{t-1})$ and $w_t = \mathbb{E}(u_t | \mathcal{F}_{t-1}) - \mathbb{E}(u_t)$. Once again, results identical to eq. (6.6) and eq. (6.7) hold true here as well. These can be proved following similar idea as before and are omitted. Further, simple calculations show that

$$\frac{1}{nb_n} \sum_{t=1}^n \mathbb{E}(u_t) \rightarrow b_n^2 \psi_K(\mu''(x)g(x) + 2\mu'(x)g'(x)), \quad (6.10)$$

as $n \rightarrow \infty$. This, along with the previous results, imply that $B(x; b_n) - \delta(x; b_n) \rightarrow 0$ in probability.

As a last piece of the proof, we use the fact that $r(x; b_n) \rightarrow 1$ for all x as $n \rightarrow \infty$. This is a well known result and has been discussed in multiple papers. Combining the asymptotic properties of $S(x; b_n)$, $B(x; b_n)$ and $r(x; b_n)$, we get the desired result. \square

Proof of Theorem 2.3. Similar to the previous proof, we start from the fact that

$$\hat{\sigma}^2(x; b_n) = \frac{1}{nb_n \hat{g}(x; b_n)} \sum_{t=1}^n K_2 \left(\frac{x - \mathbf{X}_t}{b_n} \right) (\mu(\mathbf{X}_t) + \sigma(\mathbf{X}_t)e_t - \hat{\mu}^*(\mathbf{X}_t; b_n))^2. \quad (6.11)$$

Let us define $S(x; b_n)$ in the same way as in eq. (6.2), with $K(\cdot)$ therein replaced by $K_2(\cdot)$. Let

$$S_1(x; b_n) = \frac{1}{nb_n \hat{g}(x; b_n)} \sum_{t=1}^n K_2 \left(\frac{x - \mathbf{X}_t}{b_n} \right) \sigma(\mathbf{X}_t)e_t, \quad (6.12)$$

$$S_2(x; b_n) = \frac{1}{nb_n \hat{g}(x; b_n)} \sum_{t=1}^n K_2 \left(\frac{x - \mathbf{X}_t}{b_n} \right) \sigma^2(\mathbf{X}_t)e_t^2. \quad (6.13)$$

Then, following the proof of asymptotic normality of $S(x; b_n)$ in Theorem 2.2 and using Corollary 2.1, it can be argued that uniformly for all x ,

$$\hat{\mu}^*(x; b_n) - \mu(x) = D_n + d_n, \text{ where } D_n = S_1(x; b_n) = O((nb_n)^{-1/2}), \text{ and } d_n = o((nb_n)^{-1/2}). \quad (6.14)$$

Combining eq. (6.11) and eq. (6.14), it is straightforward to note that $\hat{\sigma}^2(x; b_n)$ is asymptotically equivalent to $S_2(x; b_n)$. Next, in view of $\mathbb{E}(e_t^2) = 1$, we can write

$$\begin{aligned} S_2(x; b_n) - \sigma^2(x) &= \frac{1}{nb_n \hat{g}(x; b_n)} \sum_{t=1}^n K_2 \left(\frac{x - \mathbf{X}_t}{b_n} \right) \{ \sigma^2(\mathbf{X}_t)e_t^2 - \sigma^2(x) \} \\ &= \frac{1}{nb_n \hat{g}(x; b_n)} \sum_{t=1}^n K_2 \left(\frac{x - \mathbf{X}_t}{b_n} \right) \sigma^2(\mathbf{X}_t) \{ e_t^2 - \mathbb{E}(e_t^2) \} + \\ &\quad \frac{1}{nb_n \hat{g}(x; b_n)} \sum_{t=1}^n K_2 \left(\frac{x - \mathbf{X}_t}{b_n} \right) \{ \sigma^2(\mathbf{X}_t) - \sigma^2(x) \}. \end{aligned} \quad (6.15)$$

For the first term above, using $a_n = nb_n / \log n$, let us write

$$\begin{aligned} K_2 \left(\frac{x - \mathbf{X}_t}{b_n} \right) \sigma^2(\mathbf{X}_t) \{ e_t^2 - \mathbb{E}(e_t^2) \} &= K_2 \left(\frac{x - \mathbf{X}_t}{b_n} \right) \sigma^2(\mathbf{X}_t) \{ e_t^2 \mathbb{I}\{e_t^2 > a_n\} - \mathbb{E}(e_t^2 \mathbb{I}\{e_t^2 > a_n\}) \} \\ &\quad + K_2 \left(\frac{x - \mathbf{X}_t}{b_n} \right) \sigma^2(\mathbf{X}_t) \{ e_t^2 \mathbb{I}\{e_t^2 \leq a_n\} - \mathbb{E}(e_t^2 \mathbb{I}\{e_t^2 \leq a_n\}) \}. \end{aligned} \quad (6.16)$$

Denote the above two terms as $T_{1,t}(x; b_n)$ and $T_{2,t}(x; b_n)$. Let $T_1(x; b_n) = \sum_{t=1}^n T_{1,t}(x; b_n)$ and $T_2(x; b_n) = \sum_{t=1}^n T_{2,t}(x; b_n)$. It is easy to note that $\{T_{1,t}(x; b_n)\}_{t=1}^n$ forms martingale difference sequence with respect to the filtration \mathcal{G}_t . Also, $\mathbb{E}[e_t^4 \mathbb{I}\{e_t^2 > a_n\}]$ is $O(1)$. Thus, $\|T_1(x; b_n)\|^2 = O(nb_n)$

and $\|\partial T_1(x; b_n)/\partial x\|^2 = O(n/b_n)$, thereby implying that $\mathbb{E}[\sup_x |T_1(x; b_n)|^2] = O(n/b_n)$ and that $\sup_x |T_1(x; b_n)| = O(\sqrt{n/b_n})$.

On the other hand, $\{T_{2,t}(x; b_n)/a_n\}_{t=1}^n$ is a uniformly bounded martingale difference sequence with respect to the filtration \mathcal{G}_t . Following Lemma 4 of [Zhao and Wu \[2006\]](#), it can be argued that $\sup_x |T_2(x; b_n)| = O(\sqrt{nb_n \log n})$. Using this, in conjunction with the above result for $T_1(x; b_n)$, we get that the first term in eq. (6.15) is $O(\sqrt{1/nb_n^3} + \sqrt{\log n/nb_n})$.

For the second term in eq. (6.15), recall the expression for $B(x; b_n)$ from eq. (6.3), and note that in proving the asymptotic result of $B(x; b_n)$, we only used the properties of $\mu(\cdot)$ given by Assumption 6, all of which are true for $\sigma^2(\cdot)$ as well. Thus, exactly similar result can be proved if we replace $\mu(\cdot)$ by $\sigma^2(\cdot)$ in that expression. In particular, we can show that

$$\frac{1}{nb_n \hat{g}(x; b_n)} \sum_{t=1}^n K_2 \left(\frac{x - \mathbf{X}_t}{b_n} \right) \{ \sigma^2(\mathbf{X}_t) - \sigma^2(x) \} - \delta_\sigma(x; b_n) \rightarrow 0, \quad (6.17)$$

where $\delta_\sigma(x; b_n) = b_n^2 \psi_K (2\sigma(x)\sigma''(x) + 2(\sigma'(x))^2 + 4\sigma(x)\sigma'(x)g'(x)/g(x))$. Now, using the assumptions about the bandwidth function b_n , it is easy to see that both terms in eq. (6.15) converge to 0 as $n \rightarrow \infty$ and that concludes our proof. \square

7 Additional simulation results

In our simulation study, we use four different data generating processes (DGP), as given by Table 1. The results corresponding to two of the DGPs are presented in the main paper. Here, we focus on the other two processes. Note that NLQRM refers to the DGP where $\mu(\mathbf{X}_t)$ is nonlinear in \mathbf{X}_t and $\sigma(\mathbf{X}_t)$ is constant whereas NLHQRM denotes the process with nonlinear $\mu(\mathbf{X}_t)$ and non-constant $\sigma(\mathbf{X}_t)$. Recall that we run 1000 simulations for every DGP and for every such experiment, the root mean squared error (RMSE) of the fitted values, that is the square root of the mean of $(\hat{\mu}(x) - \mu(x))^2$ over all x in the training set, is computed. The mean RMSE corresponding to NLQRM for the three candidate models for different cases are presented in Table 10 and the same for NLHQRM are displayed in Table 11. In all the following results, KB corresponds to the method proposed by [Koenker and Bassett Jr \[1978\]](#) (refer to eq. (2.4) in the main paper), JS is the approach proposed by [Jana and Sengupta \[2019\]](#) (refer to eq. (2.5) in the main paper), and NP stands for our proposed approach (see eq. (2.11) in the main paper).

In both of these tables, we can see that the NP method records better RMSE than KB or JS methods. For the proposed nonparametric approach, the RMSE decreases with more replicates, but the values are more or less stable for different values of n . For our method, this is in line with what we observed for SQRM or GQRM (refer to the main paper). Interestingly, KB or JS do not display similar behavior and the RMSE values are always similar. It is clear that for a nonlinear mean function, these two approaches cannot perform well. It is also worth noting that for higher quantile ($\tau = 0.95$), the error increases marginally for all of the methods.

Next, we look at the prediction RMSE in different cases. Results for NLQRM are displayed in Table 12 and the same for NLHQRM are shown in Table 13. Once again, we observe that the errors are less for our proposed nonparametric approach than the other two methods. The difference is more for the lower quantiles and is less for the 95% quantile.

As a final piece in this analysis, to better understand the efficiency of the proposed approach, we focus on $n = 100$, and take a look at the prediction MSE for all future time-points (1-step ahead to 20-steps ahead). These results, for different values of K and τ , are plotted in Figure 5 (for SQRM), Figure 6 (for NLQRM), Figure 7 (for NLHQRM) and Figure 8 (for GQRM).

A similar story as before arises out of these plots. For SQRM, note that the prediction RMSE decreases as the number of replicates per time point is increasing and the prediction accuracy is less

Table 10: Empirical RMSE (mean taken over 1000 simulations) of fitted quantiles using the three different approaches for different values of τ , K and n , when the data are generated from a NLQRM.

τ	Method	$n=30$			$n=50$			$n=100$		
		$K=50$	$K=100$	$K=500$	$K=50$	$K=100$	$K=500$	$K=50$	$K=100$	$K=500$
0.7	KB	1.033	1.026	1.026	1.048	1.029	1.022	1.044	1.041	1.039
	JS	0.995	0.989	0.987	1.009	0.992	0.986	1.006	1.004	1.001
	NP	0.184	0.140	0.099	0.189	0.144	0.101	0.193	0.148	0.104
0.8	KB	1.088	1.069	1.061	1.085	1.089	1.069	1.096	1.090	1.077
	JS	1.003	0.988	0.980	1.003	1.006	0.990	1.011	1.007	0.998
	NP	0.197	0.149	0.103	0.203	0.152	0.106	0.206	0.157	0.109
0.9	KB	1.185	1.171	1.151	1.188	1.178	1.155	1.204	1.187	1.169
	JS	1.010	0.998	0.984	1.010	1.006	0.990	1.019	1.012	1.003
	NP	0.228	0.171	0.114	0.234	0.176	0.117	0.236	0.179	0.120
0.95	KB	1.309	1.258	1.245	1.320	1.283	1.251	1.314	1.291	1.264
	JS	1.029	0.998	0.988	1.032	1.011	0.996	1.025	1.016	1.003
	NP	0.261	0.202	0.130	0.268	0.206	0.135	0.273	0.212	0.139

Table 11: Empirical RMSE (mean taken over 1000 simulations) of fitted quantiles using the three different approaches for different values of τ , K and n , when the data are generated from a NLHQRM.

τ	Method	$n=30$			$n=50$			$n=100$		
		$K=50$	$K=100$	$K=500$	$K=50$	$K=100$	$K=500$	$K=50$	$K=100$	$K=500$
0.7	KB	1.062	1.045	1.030	1.065	1.047	1.034	1.075	1.062	1.042
	JS	1.047	1.032	1.017	1.049	1.033	1.022	1.059	1.047	1.030
	NP	0.254	0.185	0.122	0.257	0.191	0.124	0.263	0.195	0.129
0.8	KB	1.100	1.082	1.064	1.111	1.086	1.072	1.118	1.100	1.082
	JS	1.044	1.030	1.013	1.052	1.032	1.022	1.057	1.044	1.032
	NP	0.270	0.198	0.128	0.278	0.205	0.132	0.282	0.208	0.136
0.9	KB	1.219	1.174	1.142	1.219	1.189	1.156	1.227	1.185	1.158
	JS	1.066	1.037	1.014	1.068	1.051	1.027	1.070	1.046	1.030
	NP	0.312	0.233	0.146	0.323	0.238	0.152	0.331	0.242	0.154
0.95	KB	1.359	1.285	1.250	1.346	1.292	1.251	1.354	1.305	1.263
	JS	1.097	1.046	1.029	1.088	1.055	1.033	1.084	1.058	1.040
	NP	0.360	0.277	0.174	0.374	0.286	0.178	0.380	0.291	0.182

for higher quantiles. Here, the three methods perform similarly (RMSE ranges between 0.1 and 0.4) for all steps ahead. On the contrary, when the data are generated from any of the other three DGPs, our approach shows much better results than KB and JS. Prediction RMSE for all cases are less than 0.5 for the NP method whereas in KB and JS, the numbers are more than double of that. It can also be observed that, for all of the first three DGPs, there is a discernible difference between the performances of KB and JS methods in higher quantiles. Usually, JS performs better for $\tau = 0.95$. For GQRM though, this difference is not present. On the other hand, the nonparametric approach consistently beat the two competing methods and shows less prediction error in all steps ahead in all DGPs. This corroborates the findings of the main paper that any deviation from the assumptions of SQRM affects the performance of the two standard approaches.

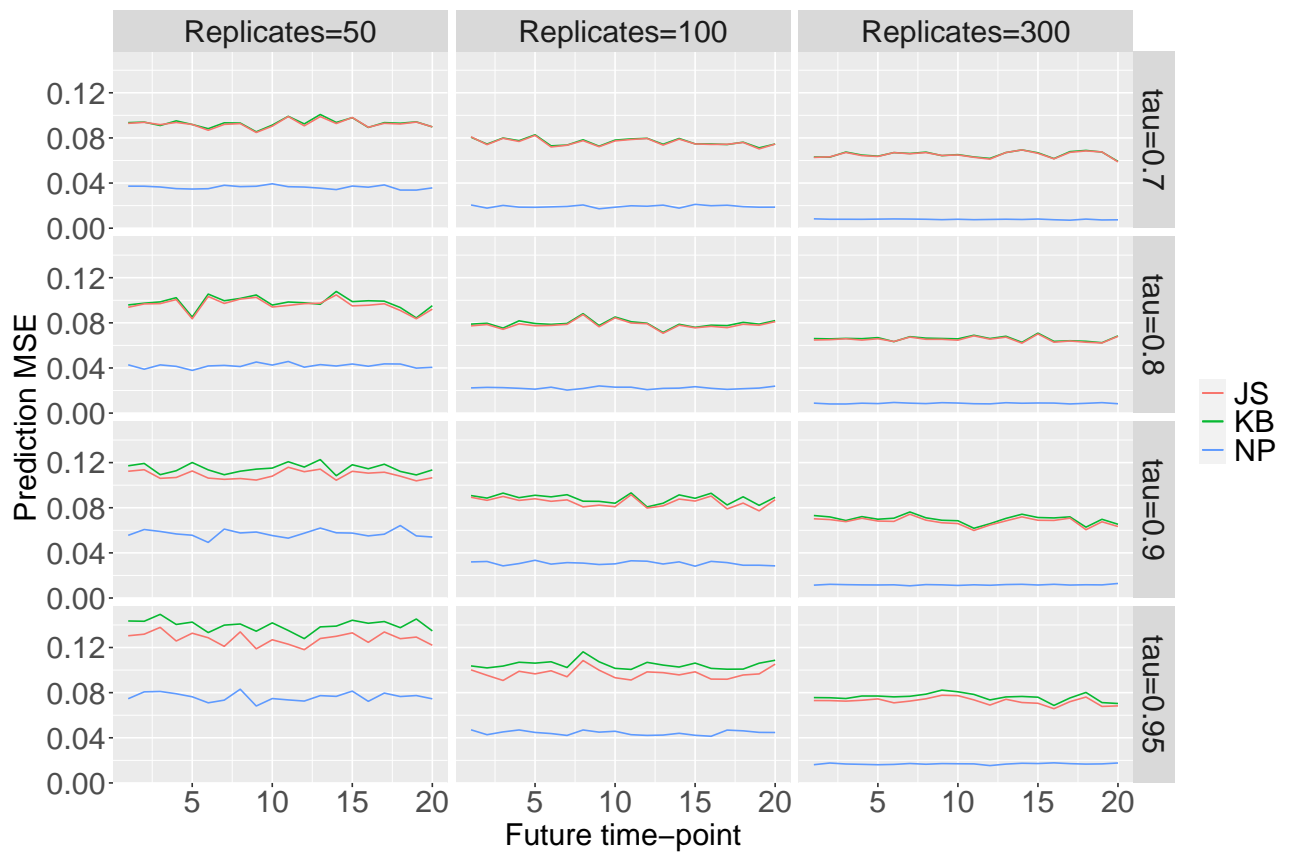
Table 12: Prediction RMSE (mean taken over 1000 simulations) for the three different approaches for different values of τ , K and n , when the data are generated from a NLQRM.

τ	Method	$n=30$			$n=50$			$n=100$		
		$K=50$	$K=100$	$K=500$	$K=50$	$K=100$	$K=500$	$K=50$	$K=100$	$K=500$
0.7	KB	1.085	1.085	1.074	1.070	1.061	1.048	1.069	1.065	1.047
	JS	1.055	1.042	1.044	1.028	1.029	1.015	1.029	1.028	1.012
	NP	0.223	0.175	0.136	0.211	0.167	0.123	0.208	0.161	0.117
0.8	KB	1.143	1.106	1.116	1.111	1.103	1.112	1.107	1.098	1.091
	JS	1.053	1.034	1.038	1.036	1.030	1.029	1.024	1.016	1.015
	NP	0.234	0.184	0.139	0.228	0.177	0.132	0.221	0.170	0.123
0.9	KB	1.222	1.200	1.202	1.219	1.199	1.186	1.213	1.193	1.171
	JS	1.058	1.033	1.031	1.039	1.028	1.017	1.034	1.022	1.011
	NP	0.270	0.205	0.158	0.259	0.200	0.143	0.252	0.190	0.135
0.95	KB	1.327	1.301	1.278	1.346	1.299	1.270	1.327	1.298	1.282
	JS	1.068	1.044	1.022	1.060	1.035	1.021	1.037	1.022	1.020
	NP	0.308	0.237	0.161	0.297	0.230	0.157	0.288	0.224	0.153

Table 13: Prediction RMSE (mean taken over 1000 simulations) for the three different approaches for different values of τ , K and n , when the data are generated from a NLHQRM.

τ	Method	$n=30$			$n=50$			$n=100$		
		$K=50$	$K=100$	$K=500$	$K=50$	$K=100$	$K=500$	$K=50$	$K=100$	$K=500$
0.7	KB	1.113	1.069	1.097	1.090	1.098	1.062	1.074	1.068	1.059
	JS	1.101	1.058	1.085	1.074	1.084	1.051	1.059	1.053	1.047
	NP	0.289	0.221	0.159	0.287	0.218	0.145	0.275	0.206	0.142
0.8	KB	1.168	1.140	1.124	1.152	1.126	1.100	1.124	1.103	1.120
	JS	1.115	1.088	1.073	1.092	1.074	1.053	1.065	1.049	1.068
	NP	0.319	0.234	0.167	0.304	0.229	0.153	0.296	0.221	0.152
0.9	KB	1.261	1.225	1.191	1.234	1.208	1.183	1.236	1.202	1.174
	JS	1.113	1.092	1.062	1.090	1.080	1.059	1.084	1.061	1.047
	NP	0.360	0.272	0.182	0.352	0.263	0.172	0.343	0.258	0.167
0.95	KB	1.378	1.328	1.287	1.375	1.324	1.277	1.378	1.310	1.271
	JS	1.129	1.099	1.077	1.120	1.083	1.061	1.106	1.072	1.054
	NP	0.408	0.322	0.210	0.404	0.314	0.199	0.399	0.305	0.195

Figure 5: Prediction MSE (mean taken over 1000 simulations) corresponding to different future time-points for the three different approaches. Data are generated from a SQRM with $n = 100$, and the results are shown for different values of τ and K .



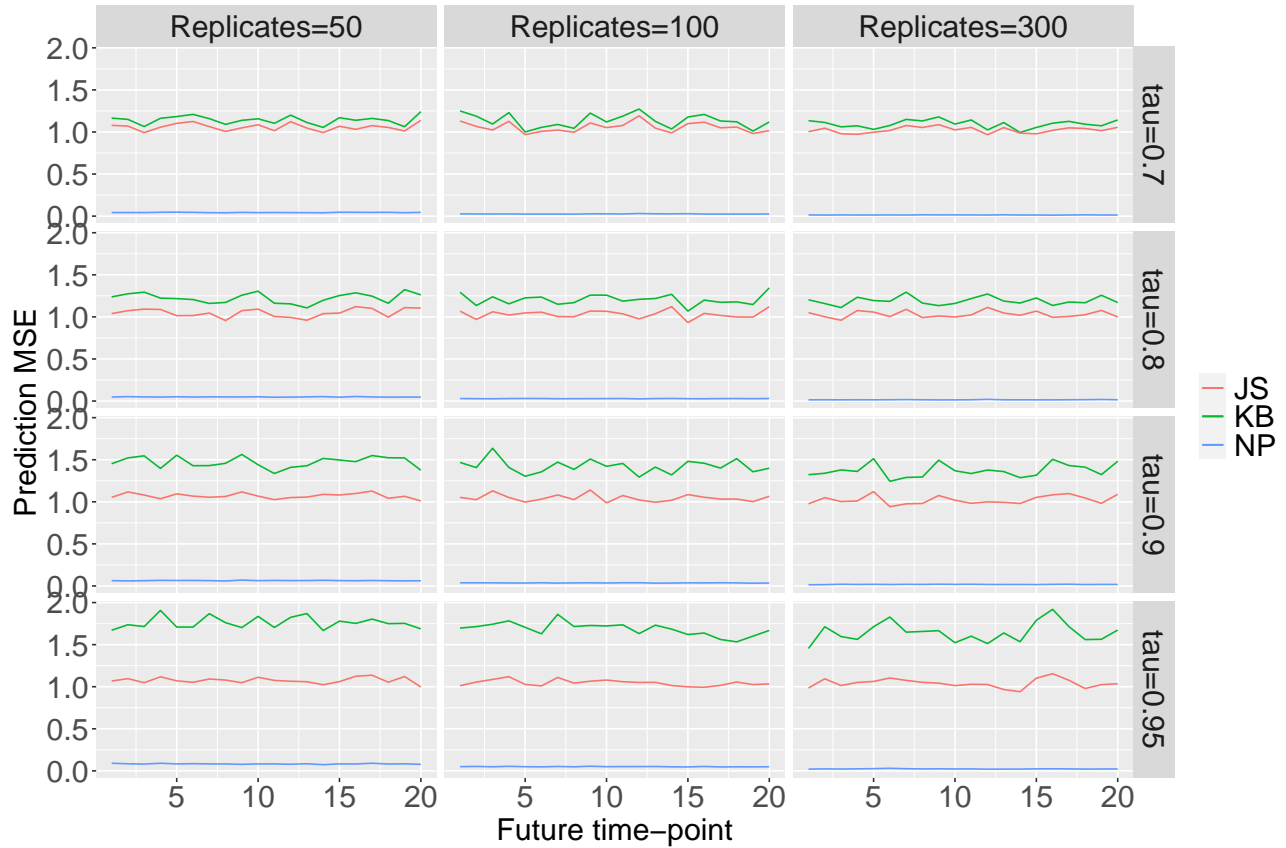


Figure 6: Prediction MSE (mean taken over 1000 simulations) corresponding to different future time-points for the three different approaches. Data are generated from a NLQRM with $n = 100$, and the results are shown for different values of τ and K .

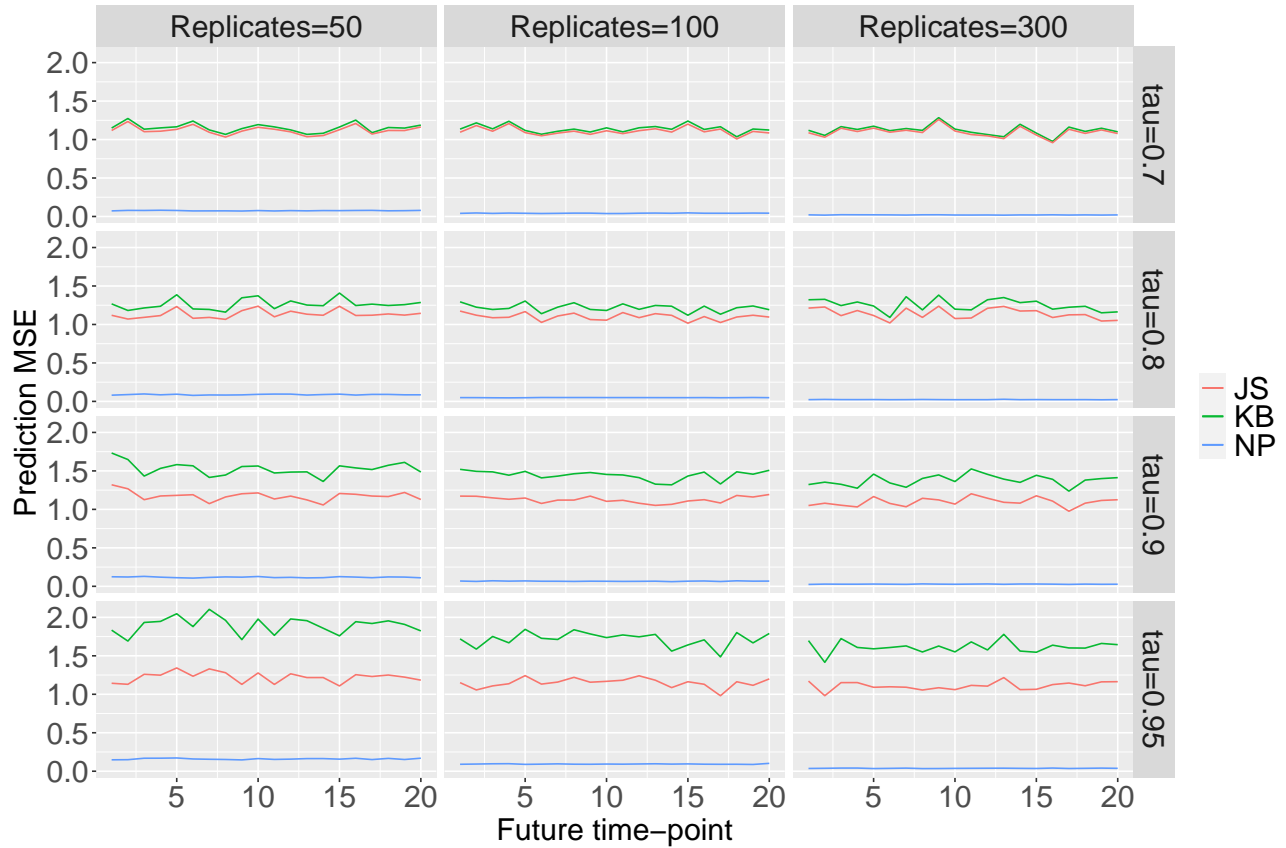


Figure 7: Prediction MSE (mean taken over 1000 simulations) corresponding to different future time-points for the three different approaches. Data are generated from a NLHQRN with $n = 100$, and the results are shown for different values of τ and K .

Figure 8: Prediction MSE (mean taken over 1000 simulations) corresponding to different future time-points for the three different approaches. Data are generated from a GQRM with $n = 100$, and the results are shown for different values of τ and K .

